Lithos 388–389 (2021) 106059

Contents lists available at ScienceDirect

Lithos

journal homepage: www.elsevier.com/locate/lithos

Research Article

A combined geochemical, Nd, and stable Ca isotopic investigation of provenance, paleo-depositional setting and sub-basin connectivity of the Proterozoic Vindhyan Basin, India

Pallabi Basu, Anupam Banerjee [1], Ramananda Chakrabarti *

Centre for Earth Sciences, Indian Institute of Science, Bangalore 560012, India

ARTICLE INFO

Article history:
Received 18 August 2020
Received in revised form 31 January 2021
Accepted 4 February 2021
Available online 18 February 2021

Keywords:
Mid-Proterozoic sediments
Vindhyan Basin
Provenance
Paleo-depositional environment
Inter-basinal correlation
Trace elements and Nd and Ca isotopes

ABSTRACT

Geochemical and isotopic investigation of Proterozoic clastic and chemical sedimentary rocks provide insights into surface conditions of the early Earth. The mid-Proterozoic Vindhyan Basin of central India, comprising ~5 km thick, mostly undeformed and unmetamorphosed clastic and chemical sediments, is one such archive which is exposed in two sub-basins, the Son Valley Vindhyan sub-basin in the east (SVV) and Chambal Valley Vindhyan sub-basin in the west (CVV). Geochemical and Nd isotopic compositions of siliciclastic sedimentary rocks from the CVV sub-basin are reported in order to understand the provenance of the Vindhyan sediments in this sub-basin and the results are compared with the provenance of the sediments exposed in the SVV sub-basin to evaluate whether the two sub-basins had shared a common provenance. Elemental ratios, such as Th/Co, La/Sc suggest that the clastic sedimentary rocks from the CVV have dominantly upper crustal silicic/felsic provenances and are broadly similar to those of equivalent stratigraphic horizons from the SVV. Initial Nd isotopic composition ($\varepsilon_{Nd(t)}$) of the siliciclastic rocks from the Lower Vindhyans of the CVV, calculated at their respective times of deposition, suggest sediment derivation from the Banded Gneissic Complex, Berach Granitoids, 1.82 Ga continental arc granitoids of the Aravalli Range and the Hindoli Volcanics. In contrast, the $\varepsilon_{Nd(t)}$ values of the Upper Vindhyan siliciclastics suggest that the Delhi Belt granitoids were the primary source of detritus during the deposition of these sediments. Paleo-depositional environment and connectivity between the SVV and CVV sub-basins are evaluated using geochemical, radiogenic Nd, and stable Ca isotopic compositions of carbonates from both sub-basins. Non-redox sensitive REY anomalies and Y/Ho ratios of carbonates from the two sub-basins suggest deposition in an epeiric sea with limited connection to the open ocean. Neodymium isotopic compositions of the carbonate units suggest that the two sub-basins were connected during the deposition of both Lower and Upper Vindhyan sediments. Carbonates from both sub-basins record a significant shift towards more radiogenic Nd isotopic compositions around 1.6 Ga, possibly as a result of an Andean-type arc magmatism in near vicinity of the Son Valley sub-basin. The $\delta^{44/40}$Ca compositions of the SVV carbonates are typically lower than the CVV carbonates. This difference is likely due to greater freshwater input in the SVV sub-basin which is consistent with the existence of paleo-gradients in the Vindhyan Basin.

1. Introduction

Drastic environmental changes during the Paleoproterozoic (Great Oxidation Event, GOE) and the Neoproterozoic (Neoproterozoic Oxidation Event, NOE) significantly modified the biogeochemical cycles on the Earth's surface (e.g., Och and Shields-Zhou, 2012). In contrast, the mid-Proterozoic (1.8 Ga–0.8 Ga) was a period of tectonic and climatic stability (e.g., Cawood and Hawkesworth, 2014) and is labelled as the 'boring billion' (Brasier and Lindsay, 1998). The 'boring billion' is characterized by the absence of high amplitude δ^{13}C excursions in inorganic carbonates suggesting a stable marine biogeochemical cycle (Brasier and Lindsay, 1998). Additionally, eukaryotic diversification rates were sluggish, possibly due to limited oxygen production in the mid-Proterozoic oceans (e.g., Planavsky et al., 2014). Apart from being a period of climatic, biogeochemical, and evolutionary stasis, the mid-Proterozoic was characterized by lithospheric stability, which is inferred from the paucity of passive margins, absence of significant Sr isotope anomalies in the paleoseawater record, and stability of core components in the configuration of Columbia and Rodinia supercontinents (Cawood and Hawkesworth, 2014). The mid-Proterozoic also recorded development of epicontinental seas with extensive shelf sedimentation

* Corresponding author at: Centre for Earth Sciences, Indian Institute of Science, Bangalore 560012, India.
E-mail address: ramananda@iisc.ac.in (R. Chakrabarti).
[1] Present address: Department of Geology, Faculty of Science, Niigata University, Japan

https://doi.org/10.1016/j.lithos.2021.106059
0024-4937/

over the stable cratons (Gilleaudeau and Kah, 2013) and these sedimentation sites are preserved in the Kaapvaal Province, Superior Province, Pilbara Craton, Baltic Shield, and the Indian Shield.

The Indian Shield hosts a suite of intra-cratonic Proterozoic sedimentary basins that are distributed in the Western and Eastern Dharwar, Bastar, Bundelkhand, and Singhbhum cratons and are referred to as the 'Purana' basins (e.g., Basu and Bickford, 2015). The opening and closing of these basins are thought to be related to the assembly and break-up of the supercontinents Kenorland, Columbia, and Rodinia (Basu and Bickford, 2015). Among the Purana basins, the Vindhyan Basin (Fig. 1a) is the largest in size with an aerial extent of approximately 178,000 Km^2 and comprising a ~ 5 km thick pile of dominantly undeformed and unmetamorphosed siliciclastic and carbonate sediments belonging to four groups which from the base to the top are Semri (Lower Vindhyans), Kaimur, Rewa, and Bhander (Upper Vindhyans) (Tandon et al., 1991). The ~2.5 Ga old Bundelkhand Granite Massif occurs at the centre of the basin and divides it into two sub-basins: The Son Valley Vindhyan (SVV) sub-basin in the east and the Chambal Valley Vindhyan (CVV) sub-basin in the west (e.g., Basu and Chakrabarti, 2020) (Fig. 1a).

Radiometric age estimates suggest that sedimentation in the Vindhyan Basin commenced during the late Paleoproterozoic and continued up to early Neoproterozoic in the CVV (e.g., George et al., 2018; Gopalan et al., 2013), while in the SVV, sedimentation possibly ceased ~1000 Ma ago (Malone et al., 2008; Turner et al., 2014) (Fig. S1). Hence, the Vindhyan Basin sediments are valuable archives of paleo-depositional and paleo-redox conditions prevalent during the mid-Proterozoic and preserve valuable information about provenance and ancient tectonic activities in the Indian sub-continent. These sediments also document evidence of early life preserved in the form of trace fossils (Chakrabarti, 1990), as well as microbially mediated stromatolites (e.g., Ray et al., 2003) and carbonaceous megafossils (Kumar, 2016).

The Vindhyan sedimentary successions in CVV and SVV are considered as stratigraphically correlated based on lithological similarities, relative stratigraphic positions, and relations to unconformities (e.g., Prasad, 1984). Both sub-basins have three prominent carbonate horizons (Fig. 1b). The uppermost Bhander Limestone from the SVV shows overlapping Pb–Pb ages with that of the stratigraphically equivalent Lakheri Limestone and the overlying Balwan Limestone of the CVV suggesting contemporaneous deposition of these carbonate horizons (Gopalan et al., 2013). However, there are no similar age constraints for the older limestone horizons and hence, their stratigraphic correlation is debatable. Additionally, based on contrasting Sr and C isotopic compositions of the limestone horizons, the stratigraphic correlation of these carbonate horizons, and that of the two sub-basins in general, has been questioned (Gilleaudeau et al., 2018; Kumar et al., 2002; Ray et al., 2003). For the siliciclastic sediments, contrasting provenances

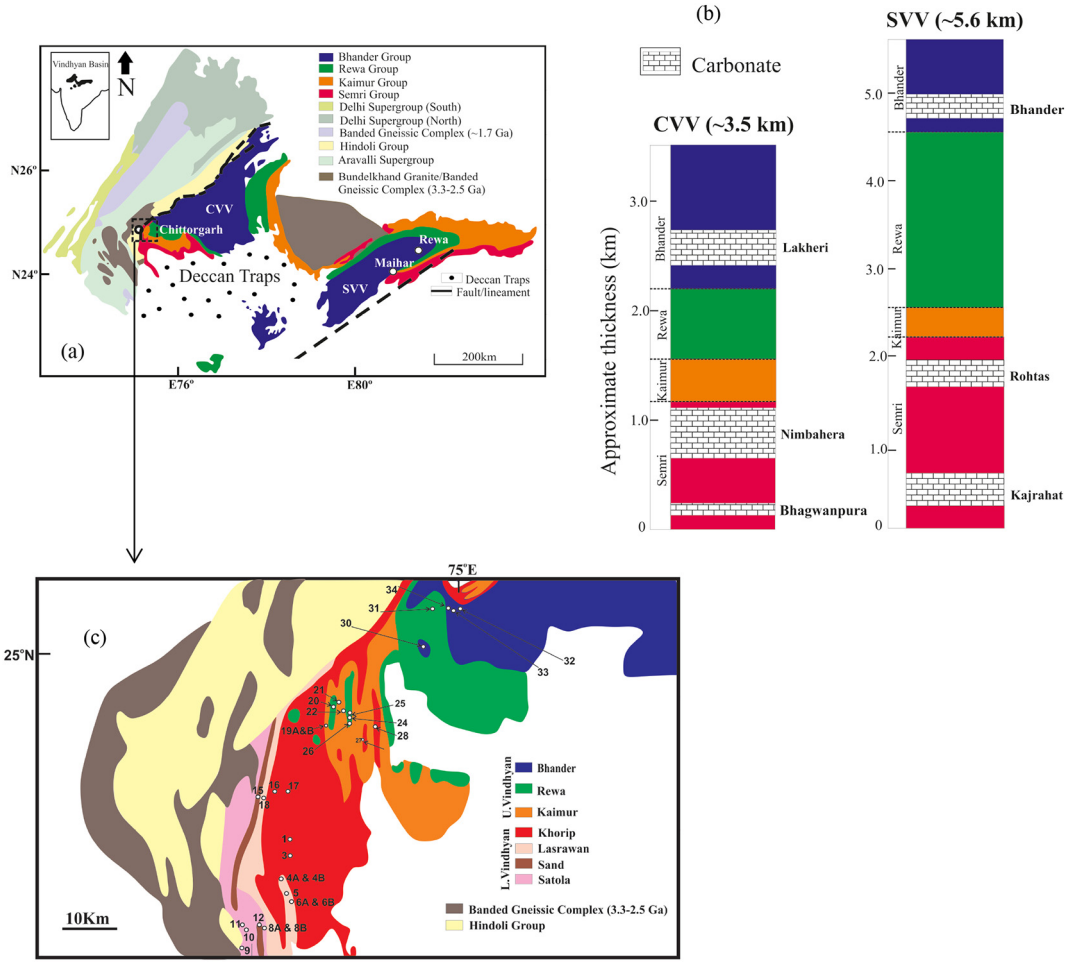

Fig. 1. (a) A generalised geological map of the Vindhyan Basin (modified after Prasad, 1984, Shukla et al., 2019) showing the Chambal Valley Vindhyan (CVV) sub-basin in the west and the Son Valley Vindhyan (SVV) sub-basin in the east separated by the Bundelkhand Granite and the spatial distribution of the Semri (Lower Vindhyan), and Kaimur, Rewa and Bhander (Upper Vindhyan) groups of rocks. (b) Simplified stratigraphy of the two sub-basins (after Shukla et al., 2019) showing three prominent carbonate horizons which are thought to be stratigraphically correlated. A detailed stratigraphy of the two Vindhyan sub-basins is shown in Fig. S1. (c) Locations of samples from the Chambal Valley Vindhyan sub-basin (CVV) analysed in this study.

have been suggested for the SVV and CVV sub-basins (e.g., Chakrabarti et al., 2007a; Shukla et al., 2019).

Paleocurrent data suggest that the SVV sediments were mostly derived from the evolving Satpura orogen towards the south with additional contributions from the Bundelkhand Granite Gneiss Complex (BGGC), Bijawar and Gwalior Group of rocks (Chakraborty, 2006) while geochemical and Nd isotope data of the SVV sediments suggest that the sediments were dominantly derived from a now extinct Andean-type arc that was located to the south of the basin (Chakrabarti et al., 2007a). Geochemical data for SVV shales further suggest that there was an influence of a basaltic source for the Upper Vindhyans (Paikaray et al., 2008). In contrast, geochemical compositions of CVV siliciclastic rocks suggest that the Archean Banded Gneissic Complex (BGC) and the BGGC occurring to the north and east of the basin, respectively, as well as the Chotanagpur Granitic Gneiss Complex (CGCC) of the Eastern Indian Shield are the main sediment sources (Raza et al., 2010; Raza et al., 2012). Additionally, Nd isotopic compositions of CVV siliciclastic rocks suggest that the Lower Vindhyan sediments were derived from the Banded Gneissic Complex (BGC) and a younger differentiated magmatic arc, while the Upper Vindhyan sediments were derived from the >1.7 Ga old rocks of the Aravalli and Delhi supergroups (Shukla et al., 2019) (Fig. 1a).

The siliciclastic sediments of inner Lesser Himalayan (iLH) sediments show similar detrital zircon age distribution as Lower and Upper Vindhyan rocks (McKenzie et al., 2011). Additionally, the ~1.6 Ga old phosphorite-bearing stromatolitic Gangolihat Dolomite of the inner Lesser Himalaya (iLH) shows similar lithological features as the Semri Group carbonates (Tirohan Dolomite). The similar detrital zircon age distribution and lithological similarities between the Vindhyan and iLH sediments suggest that they have shared a similar provenance (McKenzie et al., 2011) and hence, an overall understanding of the sediment sources of the Vindhyan Basin has implications for the provenance of the Himalayan sediments.

In this study, geochemical and isotope data for both siliciclastic and carbonate rocks are used to evaluate the evolution of the CVV and SVV sub-basins of the Vindhyan Supergroup. Elemental concentrations and Nd isotopic compositions of siliciclastic rocks from the CVV are reported and compared with those from the SVV (Chakrabarti et al., 2007a) to understand their provenances; additionally, the REY (REE + Y) compositions of the carbonate rocks from both sub-basins are reported and interpreted in terms of paleo-depositional conditions. The connectivity between the sub-basins is evaluated using radiogenic Nd and stable Ca isotopic compositions of carbonate horizons from both the CVV and SVV sub-basins.

2. Materials and methods

Siliciclastic and carbonate samples were collected from the CVV sub-basin centred around the town of Chittorgarh (Fig. 1a, c). These samples cover major stratigraphic horizons from the Lower and Upper Vindhyans and include, stratigraphically from the bottom to the top, Khardeola Sandstone and Bhagwanpura Limestone from the Satola and Sand groups, shales, sandstones and Nimbehera Limestone from the Khorip Group (Fig. S1). The Satola, Sand, and Khorip Group rocks are part of the Lower Vindhyans, equivalent to the Semri Group in the SVV (Fig. S1). From the Upper Vindhyans, samples of sandstones from the Kaimur Group, shales and sandstones from the Rewa Group, Lakheri Limestone and Bhander Sandstone from the uppermost Bhander Group were collected and analysed (Fig. S1). In addition to the sedimentary rocks from CVV, carbonate rocks from SVV, which were previously characterized for their geochemical and Nd isotopic compositions (Chakrabarti et al., 2007a), were also analysed. Additional samples of the Kajrahat, Bhagwanpura, and Lakheri limestones were obtained from the Birbal Sahni Institute of Paleosciences. All the sedimentary rocks analysed in this study are unmetamorphosed and unweathered.

Hand specimen-sized rock samples were first broken into cm-sized chips using a geological hammer, and approximately 5 g of rock chips, without any surface alteration, were ultra-sonicated with 18.2 mΩ-cm water, air-dried, and then powdered using an agate mortar and pestle. Subsequently, ~25 mg of the powdered siliciclastic samples along with selected carbonate samples were dissolved using a mixture of inorganic acids (HF + HNO_3 + HCl) for 24–40 h at 115 °C. Elemental concentrations were measured using a quadrupole inductively coupled plasma mass spectrometer (ICPMS, Thermo Scientific X-Series II) at the Center for Earth Sciences (CEaS), Indian Institute of Science (IISc), Bangalore. For whole-rock Nd isotopic measurements of these samples, approximately 100–150 mg of samples were dissolved using a combination of HF, HNO_3, and HCl. Neodymium was purified from the rock matrix using a three-step ion-exchange chromatographic separation technique followed by Nd isotopic measurements using a thermal ionization mass spectrometer (TIMS, Thermo Triton Plus) at CEaS, IISc Bangalore. Additional details of whole rock geochemcial and Nd isotopic measurements are provided in Banerjee et al. (2016).

The carbonate rocks were visually inspected to avoid surface alterations and secondary calcium carbonate veins and subsequently crushed and powdered using the same protocol as described above. To rule out the contributions of silicate detritus, carbonate samples from CVV and selected carbonate samples from the SVV (same samples analysed in Chakrabarti et al., 2007a) were treated with 10% (1.67 N) acetic acid at 80 °C, which selectively dissolves carbonates. The dissolved samples were centrifuged, and the supernatant solution was analysed for elemental concentrations using the ICPMS at CEaS, IISc. Neodymium was separated from an aliquot of the same supernatant solution using a three-step ion-exchange chromatographic procedure followed by isotopic measurements using the TIMS at CEaS, IISc. The carbonate samples from both CVV and SVV were also analysed for their stable Ca isotopic compositions. The powdered carbonate samples were dissolved using 1.5 M HCl and ~ 10 μg of Ca from the sample was mixed with specific amounts of a ^{43}Ca–^{48}Ca double spike; calcium was purified from this sample-double spike mixture using ion-exchange chromatography and subsequently analysed for isotopic measurements using the TIMS at the CEaS, IISc, following established laboratory protocols (Mondal and Chakrabarti, 2018).

3. Results

Trace element compositions of siliciclastic samples from the CVV sub-basin are reported in Table S1. All samples show light-Rare Earth Element (LREE) enriched patterns with the chondrite-normalized (CN) $(La/Yb)_{CN}$ ranging from 4.04–33; highest $(La/Yb)_{CN}$ values are observed in rocks from the Kaimur Group (Table S1, Figs. 2, 3c). All the siliciclastic rocks are characterized by negative Eu anomaly [$(Eu/Eu^* = Eu/(Sm^*Gd)^{0.5}$] with Eu/Eu* ranging from 0.38–0.83 (Table S1, Figs. 2, 3b). In the Upper Continental Crust (UCC) normalized multi-element concentration plots (Fig. 2), CVV siliciclastic rocks show enrichments in Th and U, and noticeable depletions in Ba and Sr. In both REE and UCC normalized multi-element plots (Fig. 2), gritstones from the Semri Group show lower elemental concentrations and variable patterns compared to sandstones and shales. The Th/Co values in the CVV siliciclastic rocks range from 0.02 to 66, La/Sc ranges from 1.19 to 31 and Th/Sc ranges from 0.69 to 8.6 (Table S1, Fig. 3a, d).

Neodymium isotopic compositions of representative siliciclastic samples belonging to the different stratigraphic horizons of the CVV are reported in Table S1. The measured $^{143}Nd/^{144}Nd$ ratio, expressed as $\varepsilon_{Nd(0)}$ ($\varepsilon_{Nd(0)} = [(^{143}Nd/^{144}Nd)_{sample}/(^{143}Nd/^{144}Nd)_{CHUR}-1] \times 10^4$) ranges from −25.4 to −15.4 for the Semri Group rocks (Table S1, Fig. 4a). Samples from the lowermost horizons of Semri (Satola) typically show less radiogenic $\varepsilon_{Nd(0)}$ (−25.4 to −20.6) (Table S1, Fig. 4a). Rocks from the Semri (Khorip) Group show significant variation in $\varepsilon_{Nd(0)}$ (−25.4 to −15.4). The siliciclastic rocks of the Kaimur and Rewa groups show overlapping $\varepsilon_{Nd(0)}$ ranging from −18.3 to −16.0

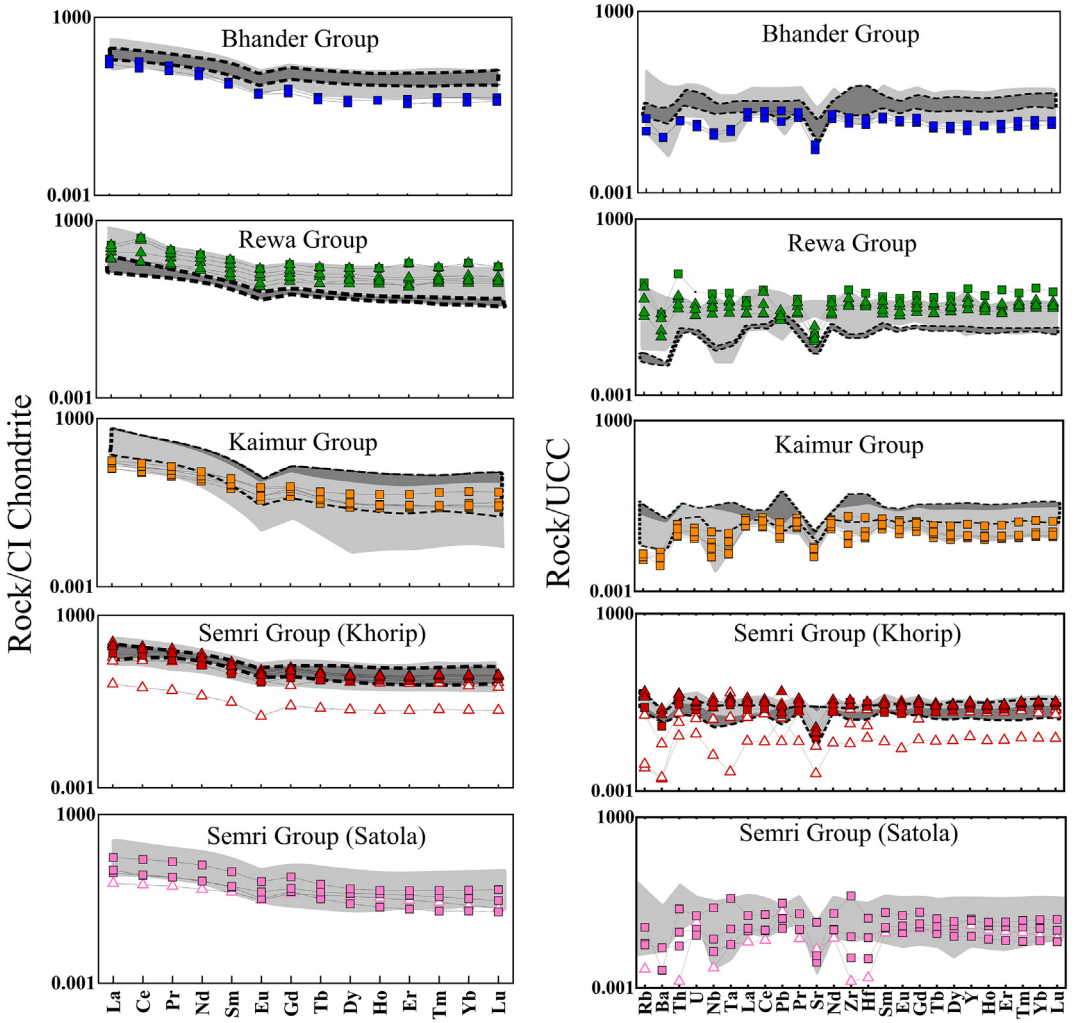

Fig. 2. CI chondrite normalized REE plot (left panel) and Upper Continental Crust (UCC) normalized multi- element plot (right panel) of siliciclastic rocks from the Semri, Kaimur, Rewa, and Bhander groups of the Chambal Valley sub-basin (CVV). The samples include gritsones (open triangles), sandstones (filled squares) and shales (filled triangles). Also shown for comparison are published geochemical data for siliciclastic sediments from the Son Valley sub-basin (SVV, darker grey shade) and CVV (light grey shade) (Chakrabarti et al., 2007a; Raza et al., 2010, 2012; Shukla et al., 2019). Chondrite and UCC data are taken from Taylor and McLennan (1985) and Rudnick and Gao (2003), respectively.

(Table S1, Fig. 4a). The $f_{Sm/Nd}$ value, which is a measure of the fractionation of Sm and Nd with respect to the bulk silicate Earth, ranges from −0.50 to −0.18 for the rocks of the Semri Group, −0.50 to −0.39 for the Kaimur Group, −0.39 to −0.33 for the Rewa Group and − 0.56 to −0.48 for the Bhander Group of rocks (Table S1, Fig. 4b). Values of the depleted mantle Nd model age (T_{DM}) range from 1.7 to 4.3 Ga (Table S1, Fig. 4c). There is a decrease in the T_{DM} values across the boundary between the Semri (2.0–4.3 Ga) and the Kaimur Group (1.8–2.2 Ga) (Fig. 4c). The Rewa Group rocks show a slight increase in T_{DM} (2.3–2.5 Ga) while the overlying Bhander Group rocks show lower T_{DM} values (1.7–2.1 Ga) (Table S1, Fig. 4c). The $\varepsilon_{Nd(t)}$ values for the different litho-units, calculated based on available sedimentation age estimates, are reported in Table S1 and shown in Figs. 4d and 5. The mean ages of the crust that provided detritus to the CVV, calculated by subtracting the depositional ages from the T_{DM}, range from 0.38–2.55 Ga (Table S1, Fig. 6).

Major and trace element compositions of acetic acid dissolved carbonate rocks from CVV and SVV are reported in Table S2. Additionally, major and trace element compositions of few carbonate units from the CVV, dissolved using inorganic acids, are also reported in Table S2 for comparison. The CVV carbonates dissolved using inorganic acids show higher concentrations of detritus associated elements (e.g., Al, Rb, Zr and Th) and total REY compared to their acetic acid dissolved counterparts (Table S2, Fig. S2a). However, the values of Y/Ho and $(La/La^*)_{SN}$ (SN = Shale Normalized) do not vary significantly between acetic acid and inorganic acid dissolved fractions (Figs. S2b, S2c). As whole rock dissolution process resulted in higher concentrations of detritus associated elements, only the data from the acetic acid dissolved carbonate rocks are used for further discussions on paleo-depositional environment and sub-basin connectivity. The Bhagwanpura Limestone shows relatively high Mg/Ca ratio (0.008 to 0.56), while the Kajrahat, Rohtas, Nimbahera, Lakheri and Bhander limestones show lower Mg/Ca (~0.003–0.014). The Bhagwanpura Limestone samples also show high Mn/Sr (12.0–47.1) and Fe/Sr (49.4–140.2) while the other limestone horizons show relatively low Mn/Sr (0.1–21.9) and Fe/Sr (2.1–41) (Table S2). In Post Archean Australian Shale (PAAS) normalized REY plots (Fig. 7), the Vindhyan carbonates show moderate HREE enrichment with $(Pr/Yb)_{SN}$ (SN = Shale Normalized) ranging from 0.48–1.04 (Table S2). The REY anomalies are calculated as: $La/La^* = La/(3Pr-2Nd)$; $Ce/Ce^* = Ce/(2Pr-Nd)$, $Gd/Gd^* = Gd/(2\ Tb-Dy)$ (Bolhar et al., 2004). The Vindhyan carbonates show $(La/La^*)_{SN}$ values from 0.88–1.62, $(Gd/Gd^*)_{SN}$ from 0.94–1.20, $(Ce/Ce^*)_{SN}$ from 0.80–1.06, and superchondritic Y/Ho values ranging from 28 to 40- (Table S2, Figs. 7, 8). One limestone sample from the Rohtas Formation shows high Y/Ho (54) as well as positive La and Gd anomalies (Figs. 7, 8).

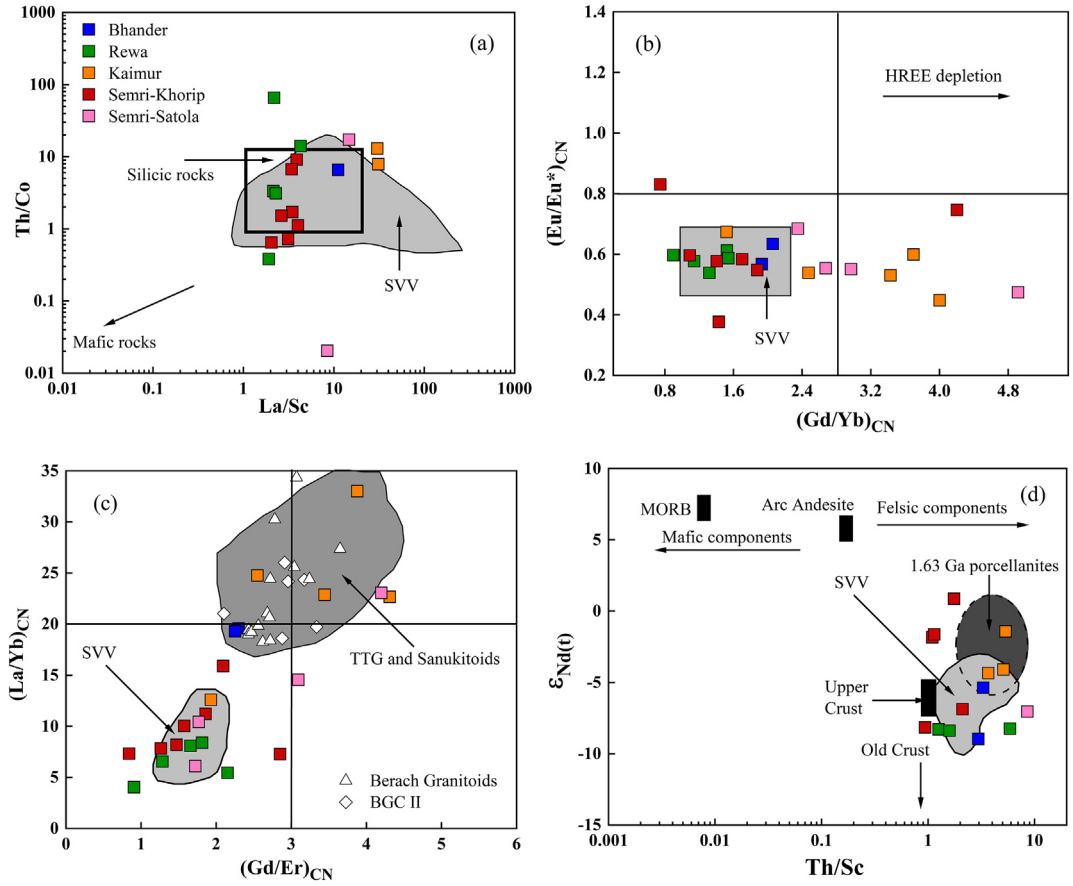

Fig. 3. Elemental ratios and initial Nd isotopic compositions ($\varepsilon Nd_{(t)}$) of siliciclastic rocks from the Chambal Valley sub-basin (CVV, coloured squares) are plotted along with rocks from the Son Valley sub-basin (SVV, dark grey field) for comparison. The SVV data are taken from Chakrabarti et al. (2007a). (a) In the plot of Th/Co vs. La/Sc (modified after Cullers, 2002), the CVV (barring RV10) and SVV rocks show overlapping compositions, both suggesting derivation from a silicic provenance (open black rectangle). (b) In the plot of $(Eu/Eu^*)_{CN}$ vs. $(Gd/Yb)_{CN}$, the CVV and SVV siliciclastic rocks show similar Eu/Eu* values, while some of the CVV rocks show higher $(Gd/Yb)_{CN}$. (c) In the plot of $(La/Yb)_{CN}$ vs. $(Gd/Er)_{CN}$, Kaimur Group of rocks from the CVV show higher LREE and HREE fractionation compared to SVV rocks. Interestingly, the compositions of the Kaimur Group of rocks from the CVV overlap with the compositions of global TTGs (data compiled from Halla et al., 2009; Moyen and Martin, 2012). These rocks also show similar geochemical signature of local basements rocks (Banded Gneissic Complex and Berach Granitoids) (Ahmad et al., 2018; Mondal and Raza, 2013). (d) In the plot of $\varepsilon_{Nd(t)}$ vs. Th/Sc (modified after McLennan et al., 1995), compositions of most CVV and SVV siliciclastic rocks overlap with that of recycled upper crust with Th/Sc >1.

Neodymium isotopic composition of the acetic acid dissolved carbonates from CVV and SVV are reported in Table S2. Whole rock Nd isotopic compositions for selected carbonate rocks from the CVV are also reported for comparison (Table S2). As the acetic acid dissolution technique results in lower concentration of detritus associated elements, Nd isotopic composition measured in carbonates dissolved using acetic acid are considered for further discussions. The $\varepsilon_{Nd(0)}$ values of the acetic acid dissolved carbonates range from −13.9 to −24.0 in the CVV (Table S2). In the SVV, $\varepsilon_{Nd(0)}$ values of the acetic acid dissolved carbonates range from −15.1 to −25.6 (Table S2). The initial Nd isotopic compositions ($\varepsilon_{Nd(t)}$) of the carbonate rocks, calculated at the estimated time of deposition of the sediments, are also reported in Table S2 and shown in Fig. 9.

Stable Ca isotope compositions of Vindhyan carbonates from Chambal Valley and Son Valley sub-basins, expressed as $\delta^{44/40}Ca_{SRM915a}$ (‰) = $(^{44/40}Ca_{sample}/^{44/40}Ca_{NIST\ SRM915a} - 1) \times 1000$, are reported in Table S3. The $\delta^{44/40}Ca_{SRM915a}$ of a solitary sample of the Kajrahat Limestone from the SVV (0.61‰) is lower than that of samples from the stratigraphically equivalent Bhagwanpura Limestone from the CVV (0.82 to 1.09‰) (Fig. 10). The $\delta^{44/40}Ca_{SRM915a}$ of Rohtas Limestone from the SVV (0.81‰) is lower compared to that of the Nimbahera Limestone from the CVV (0.97 to 1.21‰). In the Upper Vindhyans, carbonate samples from the Bhander Limestone from SVV also show lower $\delta^{44/40}Ca_{SRM915a}$ (0.79–0.85‰) compared to the $\delta^{44/40}Ca_{SRM915a}$ of Lakheri Limestone samples from the CVV (1.19‰) (Fig. 10).

4. Discussion

4.1. Connectivity between Chambal Valley and Son Valley sub-basins: Insights from comparative provenance study of clastic sedimentary rocks

Ancient sedimentary records preserve signatures of old continental crust that have since been eroded. Hence, studying such sediments provide information regarding the evolution of crust through time. Geochemical compositions of sedimentary rocks preserve the composition of the provenance provided the processes of weathering, transportation, and diagenesis do not alter the composition. The REEs and other immobile elements, are not affected by such processes unless, the amount of organic matter in the sediment is high (Chakrabarti et al., 2007b). Neodymium isotope compositions are also valuable indicators of sediment provenance for fine-grained sedimentary rocks, where it is generally impossible to determine the provenance petrographically (e.g., Chakrabarti et al., 2007a and references therein). Additionally, Nd isotopes also add a temporal dimension by providing extraction ages of the sediment sources from the depleted mantle (depleted mantle Nd model ages, T_{DM}). Such temporal information can complement provenance age information obtained from zircon studies in coarse-grained sedimentary rocks. While information from zircons are biased towards felsic provenance, whole rock Nd isotope compositions of clastic sediments reflect contribution from both mafic and felsic sources. In this study, trace element ratios of the siliciclastic sediments

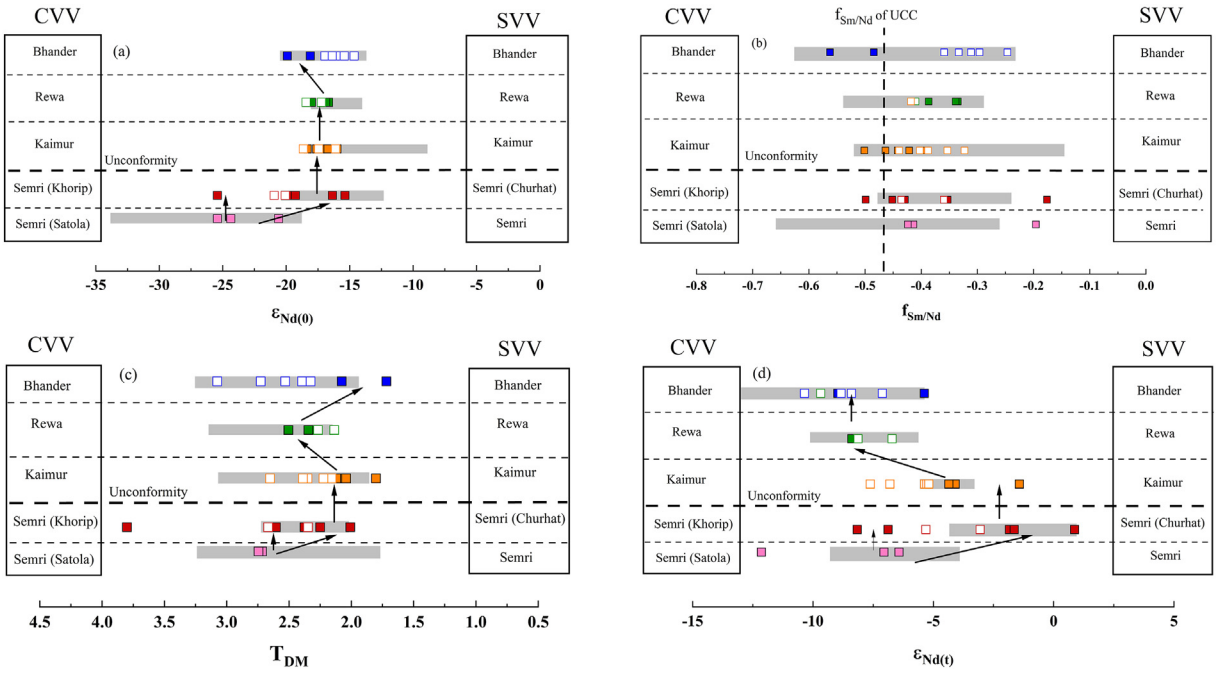

Fig. 4. (a) The present-day Nd isotopic composition ($\varepsilon_{Nd(0)}$), (b) $f_{Sm/Nd}$, (c) depleted mantle model ages (T_{DM}) and (d) initial Nd isotopic compositions ($\varepsilon_{Nd(t)}$) of siliciclastic rocks from the CVV analysed in the present study (filled squares). Also plotted for comparison are published data for the siliciclastic rocks from the CVV (shaded bars, Shukla et al., 2019) and the SVV (open squares, Chakrabarti et al., 2007a). The $\varepsilon_{Nd(t)}$ values have been calculated considering depositional ages of 0.9 Ga, 1.0 Ga, 1.21 Ga, 1.63 Ga, and 1.72 Ga for the Bhander, Rewa, Kaimur, and Semri (Khorip and Satola) groups, respectively. See text for details.

from the CVV are utilized to understand the overall composition of the provenance of these sediments; while their Nd isotope compositions are compared with those of potential provenances whose compositions are calculated at the time of depositions of the Vindhyan sediments (Fig. 5). The latter approach has been taken as the Nd isotopic compositions of different source rocks, which have evolved with different

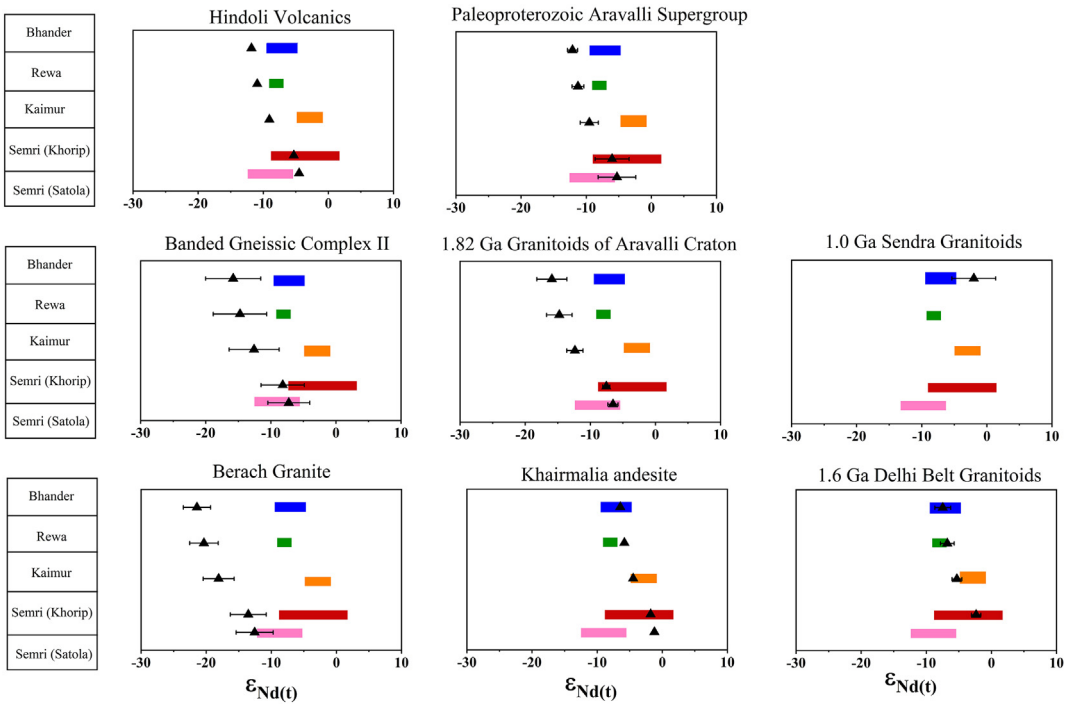

Fig. 5. Initial Nd isotopic composition ($\varepsilon_{Nd(t)}$) of the siliciclastic rocks from the CVV (shaded bars) calculated at their estimated times of deposition (t), based on available age data (see text for details). The depositional ages are considered to be 0.9 Ga, 1.0 Ga, 1.21 Ga, 1.63 Ga, and 1.72 Ga for the Bhander, Rewa, Kaimur and Semri (Khorip and Satola) groups of rocks, respectively. Also plotted for comparison are the $\varepsilon_{Nd(t)}$ of potential provenances for the CVV rocks (triangles), calculated at the estimated times of sediment deposition of the respective stratigraphic groups. Isotopic data for these rocks are taken from published literature (Chakrabarti et al., 2007a; George and Ray, 2017; Gopalan et al., 1990; Kaur et al., 2009, 2007; Pandit et al., 2003; Shukla et al., 2019). For the Lower Vindhyan sedimentary rocks, possible sediment sources are the Archean Banded Gneissic Complex (BGC), Berach Granitoids, 1.8 Ga old continental arc granitoids from the Aravalli Belt, Hindoli Volcanics and Khairmalia Andesite. For the Upper Vindhyan sedimentary rocks, contributions from older basement rocks decreased over time and the Delhi Belt granitoids became a major source of sediments.

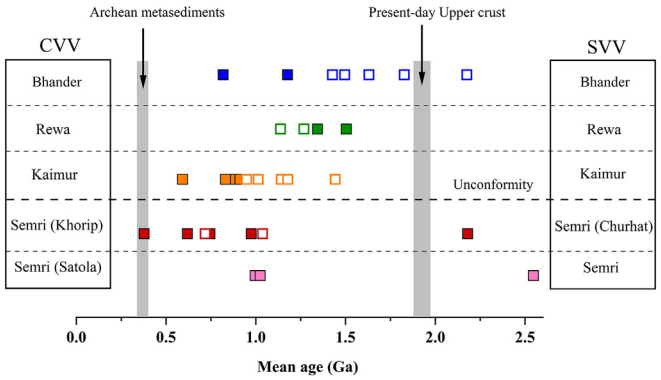

Fig. 6. Mean age of the continental crust surrounding the CVV (filled squares) and SVV (open squares) Vindhyan Basin that most likely supplied detritus to the Vindhyan siliciclastic rocks. Mean ages of Archean sediments (Garçon et al., 2017) and present-day Upper crust (Jacobsen, 1988) are shown for reference (vertical bars).

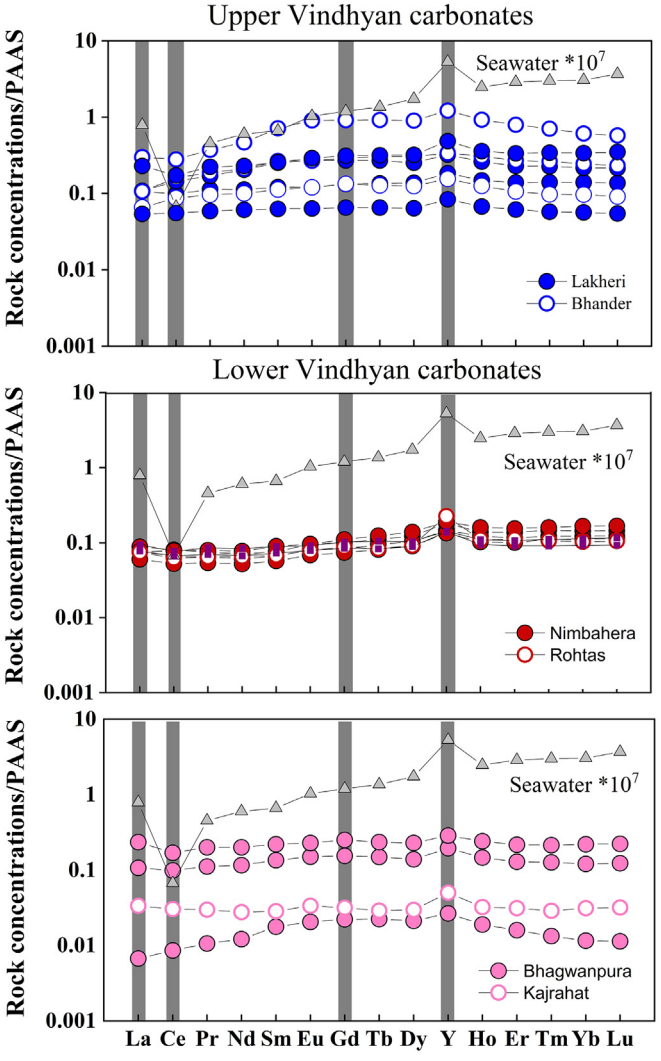

Fig. 7. Post Archean Australian Shale (PAAS)-normalized REY (REE + Y) patterns of acetic acid dissolved carbonates from the CVV (filled circles) and SVV (open circles) sub-basins. Also shown for comparison is the REY pattern of modern seawater (filled grey triangle, data from Alibo and Nozaki, 1999). Compared to modern-day seawater, the Vindhyan Basin carbonates do not show any concentration anomalies of the non-redox sensitive elements La and Gd while the Y anomalies, observed in some samples, are insignificant compared to modern seawater. See text for details.

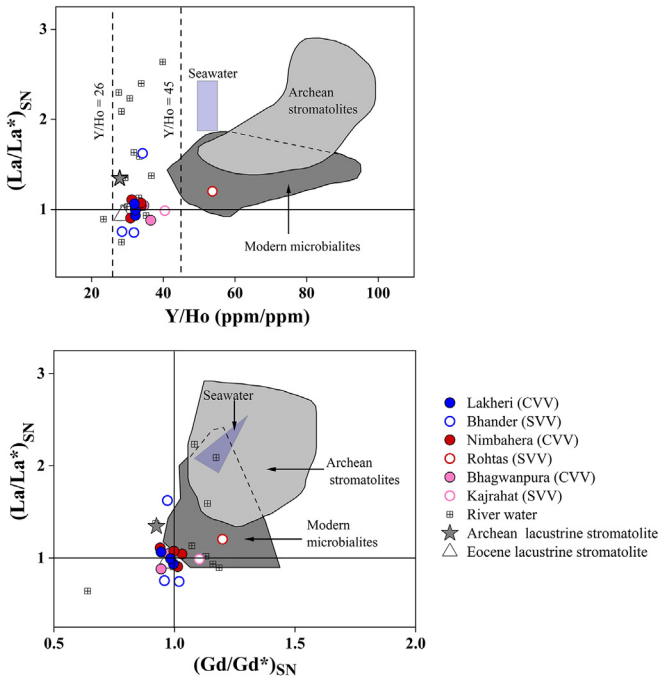

Fig. 8. In plots of $(La/La^*)_{SN}$ vs. Y/Ho (ppm/ppm) and $(La/La^*)_{SN}$ vs. $(Gd/Gd^*)_{SN}$ (SN = PAAS normalized), modern-day seawater (purple shaded region) shows positive La anomaly, Gd anomaly, and superchondritic Y/Ho, which is in contrast to the compositions of modern river water (striped squares). Relatively modern (Holocene and Devonian) microbialites (dark grey shaded region) as well as Archean stromatolites (light grey shaded region) precipitated from seawater retain this seawater signature (data from Kamber and Webb, 2001; Nothdurft et al., 2004; Van Kranendonk et al., 2003; Webb and Kamber, 2000). In contrast, Eocene stromatolites formed under lacustrine conditions (open triangle, data from Bolhar and Van Kranendonk, 2007) do not show significant positive La and Gd anomalies and display low Y/Ho (< 45). Archean stromatolites formed under lacustrine conditions also show similar non-seawater like REY signature (filled grey star, Bolhar and Kranendonk, 2007). Carbonates from both CVV (filled circles) and SVV (open circles) do not show REY signature characteristic of an open ocean thereby suggesting that these carbonates were most likely deposited in an epeiric environment with limited connection to the open ocean. (For interpretation of the references to colour in this figure legend, the reader is referred to the web version of this article.)

Sm/Nd ratios, could have the same measured Nd isotopic composition, thereby limiting the use of measured Nd isotopic compositions to accurately infer the provenance of sediments. Finally, the compositions of the CVV siliciclastic rocks are compared with those from the SVV (Chakrabarti et al., 2007a) to understand whether the CVV and SVV sub-basins had a similar provenance during their prolonged depositional history.

Potential provenances of CVV sedimentary rocks exposed around the basin whose Nd isotopic compositions were considered include the Banded Gneissic complex II (BGC-II) (George and Ray, 2017), Hindoli Volcanics, Khairmalia Andesite, Berach Granitoids and Aravalli Supergroup rocks (Shukla et al., 2019), 1.82 Ga and 1.6 Ga old Granitoids of the Aravalli region (Kaur et al., 2007; Kaur et al., 2009), granitoids from Sendra region (Pandit et al., 2003), and ~1.63 Ga old porcellanites from SVV (Chakrabarti et al., 2007a). The $\varepsilon_{Nd(1.72\ Ga)}$ composition of the Khardeola Sandstone of Satola Group, which is the lowermost siliciclastic unit in the CVV shows similarity with initial Nd isotopic compositions ($\varepsilon_{Nd(1.72\ Ga)}$) of basement rocks from the Banded Gneissic Complex II (BGC-II) and Berach Granitoids (Fig. 5). Additionally, sediments sourced from the 1.82 Ga continental arc granitoids from the Aravalli mountain range can explain the Nd isotopic compositions of relatively radiogenic end members of the Khardeola Sandstone. In the overlying Khorip Group, a large range in $\varepsilon_{Nd(1.63\ Ga)}$ composition has been observed (Fig. 5). The isotopic composition of population one ($n = 2$) with unradiogenic $\varepsilon_{Nd(1.63\ Ga)}$ and older T_{DM} (2.6–3.8 Ga)

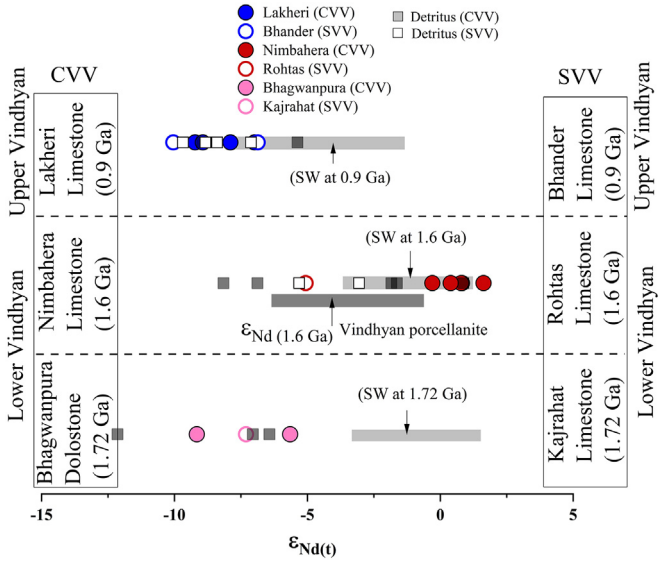

Fig. 9. Initial Nd isotopic compositions ($\varepsilon_{Nd(t)}$) calculated at their estimated times of deposition of three carbonate horizons from the CVV (filled circles) and the stratigraphically correlated carbonate horizons from the SVV (open circles). Also shown for comparison are the Nd isotopic compositions of ~1.6 Ga porcellanites exposed in the SVV (dark grey horizontal bar, Chakrabarti et al., 2007a) as well as the SVV and CVV detritus (square symbols) (Chakrabarti et al., 2007a; this study). The initial Nd isotopic composition of contemporaneous seawater (SW, light grey horizontal bar) calculated at 1.72 Ga, 1.6 Ga, 0.9 Ga is also plotted (data from Jacobsen and Pimentel-Klose, 1988). Around 1.6 Ga ago, carbonate horizons from both sub-basins recorded a significant shift in $\varepsilon_{Nd(t)}$ towards more radiogenic values consistent with increased contribution from a juvenile source, possibly from an Andean-type arc in the near vicinity of the SVV (Porcellanite, Chakrabarti et al., 2007a). See text for details.

(Table S1) can be explained by sediment derivation from older basement rocks such as the BGC and continued contribution from the continental arc granitoids (Fig. 5). The population two ($n = 3$) is compositionally similar with ~1.8 Ga Khairmalia Andesite and Hindoli Volcanics (Fig. 5). Relative contribution from these sources has also been observed from the zircon record of the Semri Group rocks from the CVV, in which zircon grains from 2.5 Ga and 1.8 Ga is dominant (McKenzie et al., 2013). The 1.6 Ga granitoid rocks from the Delhi Belt and porcellanites from the SVV show compositional similarity, however, based on absence of any ~1.6 Ga zircons in the Semri Group rocks from the CVV, possibility of sediment contribution from these sources is eliminated. The $\varepsilon_{Nd(t)}$ values of Aravalli Supergroup are also similar to those of the Lower Vindhyan sediments. However, the detrital zircon age distribution (1.7–1.9 Ga) in the lower part of the Aravalli Supergroup (Jhamarkotra Formation) suggests that the time of sedimentation of the Aravalli Supergroup is similar to or younger than the time of sedimentation of the Lower Semri Group of the Vindhyans (McKenzie et al., 2013), which makes it an unlikely source of sediments to the Lower Vindhyans (Shukla et al., 2019). Additionally, McKenzie et al. (2013) suggested that the Aravalli Supergroup is the distal equivalent of the Vindhyan Basin, which could suggest that the Lower Vindhyan and Aravalli Supergroup were receiving detritus from the same source although, sediment reworking from the Aravalli Supergroup to the Vindhyan Basin cannot be completely ruled out. The Upper Vindhyan sedimentation was initiated after a ~400 million years hiatus (Tripathy and Singh, 2015) with deposition of the Kaimur Group of rocks. Higher values of $(La/Yb)_{CN}$ and $(Gd/Er)_{CN}$ values in siliciclastic rocks from the Kaimur Group relative to those from the Semri Group (Fig. 3c) and the sudden change to lower $\varepsilon_{Nd(t)}$ values in the Kaimur Group rocks relative to the upper Semri Group rocks (Fig. 4d) suggests a significant shift in the provenance during Lower to Upper Vindhyan transition. Contribution from older basement rocks of the Aravalli Craton decreased significantly in the Upper Vindhyan rocks (Fig. 5). The Nd isotopic compositions of the Kaimur Group rocks show similarity with 1.6 Ga old granitoids from the Northern Delhi Belt (Fig. 5). In the detrital zircon record, the Kaimur Group rocks from the CVV show prominent peaks around 1.6 and 1.2 Ga (McKenzie et al., 2013). We suggest that the compositionally similar 1.6 Ga granitoids from the Delhi Belt are the source of Kaimur Group sediments (Fig. 5). As Kaimur Group and Delhi Supergroup show remarkably similar detrital zircon record, it is possible that sediments of Delhi Supergroup could have been a significant source of the Kaimur Group of rocks in the CVV. Although the Kaimur Group of rocks show TTG like compositions (Fig. 3c), their Nd isotopic compositions suggest that older basement TTG gneisses of the Aravalli Craton were not a major source of sediments. It is possible that Kaimur Group received detritus from a source with similar TTG like geochemical affinity which is not preserved. The Delhi Belt Granitoids continued to be major source of sediments during the deposition of Rewa Group (Fig. 5). During the deposition of the Bhander Group, ~1.0 Ga granitoids of the Aravalli Craton (the Sendra Granitoids) remain a major source (Fig. 5). A mixed provenance is possible for the Bhander Group of rocks as literature data show larger spread in the Nd isotopic composition (Figs. 4a, d). The $\varepsilon_{Nd(t)}$ composition of the ~1.8 Ga Khairmalia andesite (Rao et al., 2013) is similar to that of the Upper Vindhyan sediments (Fig. 5). However, the absence of ~1.8 Ga zircons in Upper Vindhyan sediments (McKenzie et al., 2013) rules out the Khairmalia andesite as a major sediment source for the Upper Vindhyans.

A comparative study based on trace element geochemistry of CVV and SVV clastic rocks suggests that sediments in both sub-basins were derived from a felsic source (Fig. 3a). The CVV siliciclastic rocks show $(Eu/Eu^*)_{CN}$ compositions similar to that of the SVV siliciclastic rocks

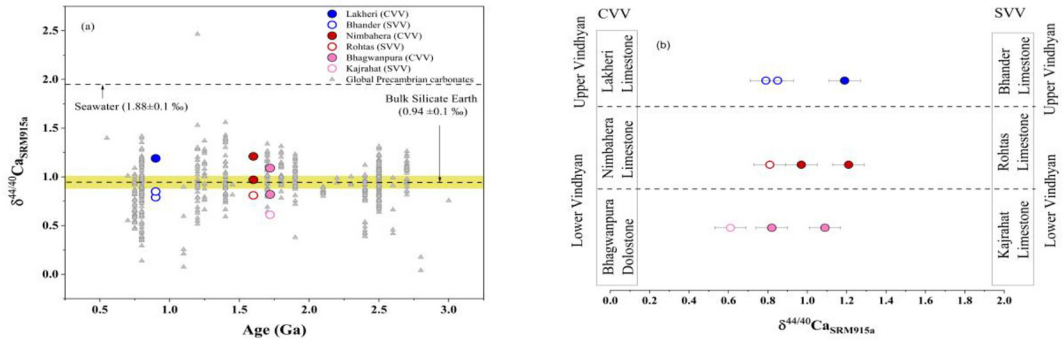

Fig. 10. (a) Stable Ca isotopic compositions ($\delta^{44/40}Ca_{SRM915a}$) of the Vindhyan carbonates from the CVV (filled circles) and SVV (open circles) overlap with those of other carbonates worldwide of the same age (grey triangles, Blättler and Higgins, 2017). (b) The $\delta^{44/40}Ca_{SRM915a}$ of the Vindhyan Basin carbonates show a large range with SVV carbonates (open circles) showing lower values than the stratigraphically equivalent CVV carbonates. The lower $\delta^{44/40}Ca$ values of the SVV carbonates suggest deposition under the increased influence of freshwater input. See text for details.

(Fig. 3b) while their absolute values (0.38–0.83) suggest derivation from differentiated igneous sources (Fig. 3b). The Kaimur Group rocks from the CVV show distinctive geochemical composition with higher $(La/Yb)_{CN}$ (12.58–33) and $(Gd/Er)_{CN}$ (1.93–4.31) compared to other clastic horizons of the Vindhyan Basin and their REE compositions are similar to global TTGs and Sanukitoids (Halla et al., 2009; Moyen and Martin, 2012; Fig. 3c). Overall, the trace element compositions of siliciclastic rocks from the CVV (barring the Kaimur Group of rocks) and SVV sub-basins are broadly similar (Fig. 3) and suggest their derivation from sources with evolved geochemical signatures. A comparative study based on Nd isotopic composition of CVV and SVV clastic rocks is presented in Fig. 4. Initial Nd isotopic compositions of the CVV clastics show large variation with $\varepsilon_{Nd(1.63\ Ga)}$ ranging from −8.2 to 0.9 (Table. S2) suggesting a mixed provenance. The Lower Vindhayn rocks from SVV show a constricted range in Nd isotopic composition. Kaimur Group of rocks from the CVV show relatively younger T_{DM} and radiogenic $\varepsilon_{Nd(1.21\ Ga)}$ compared to those in the SVV (Fig. 4c, d), which suggests sediment derivation from a younger source. A younger provenance for the Kaimur Group rocks in CVV is also suggested from detrital zircon age population, where Kaimur rocks from CVV show peaks at 1.58 Ga and 1.17 Ga, while those from the SVV show peaks at 2.5 Ga, 1.85 Ga, 1.71 Ga, and 1.17 Ga (McKenzie et al., 2013). The Kaimur Group rocks from CVV also show high $(La/Yb)_{CN}$ and $(Gd/Er)_{CN}$ values compared to those from SVV (Fig. 3c) indicating a different provenance. The Kaimur-Rewa transition is not marked by any regional unconformity; however, in the CVV, Rewa rocks show unradiogenic $\varepsilon_{Nd(1.0\ Ga)}$ ranging from −8.4 to −8.2 and an older T_{DM} of 2.3 to 2.5, which is significantly different from the Kaimur Group rocks (Fig. 4c, d). It is important to mention that $f_{Sm/Nd}$ is not constant across the Kaimur-Rewa boundary and hence the change in Nd isotopic composition could be a result of post-depositional alterations (Fig. 4b). In the SVV, Nd isotopic compositions do not show significant changes across the Kaimur-Rewa boundary (Fig. 4c, d). The T_{DM} and $\varepsilon_{Nd(0.9\ Ga)}$ of Bhander Group rocks from CVV suggest juvenile input; however, data from Shukla et al. (2019) show a large range in Nd isotopic composition and T_{DM} suggesting a mixed provenance (Figs. 4c, d). A mixed provenance is also suggested from the detrital zircon ages of Bhander Sandstone which show peaks ranging from 1.7 Ga to 1.0 Ga (McKenzie et al., 2013). The isotopic composition of Bhander Group rocks from the SVV overlaps with those from CVV suggesting sediment derivation from geochemically similar rock type.

The mean age of the Precambrian continental crust exposed to erosion is considered for both CVV and SVV to verify possible contributions from distinct sediment sources throughout their entire course of basin evolution (Fig. 6). The lower Vindhyan CVV rocks show large range in their mean ages (0.38–2.55 Ga) which suggests contribution from both older and younger sources. In the SVV, the Lower Vindhyan sedimentary rocks show relatively younger mean ages (0.72–1.04 Ga) (Fig. 6), which is consistent with a juvenile source in the near vicinity of the SVV, which provided bulk of the sediments to this sub-basin. The Upper Vindhyan rocks from the CVV show mean ages ranging from 0.59–1.5 Ga (Table S1), while the Upper Vindhyan rocks from the SVV show mean age ranging from 0.95–2.18 Ga (Fig. 6). The mean age of the sedimentary rocks in the Vindhyan Basin is higher compared to those in the Paleoproterozoic Cuddapah Basin (~0.6 Ga) (Zachariah et al., 1999) and Archean metasedimentary rocks from Barberton Group, South Africa (0.3–0.4 Ga) (Garcon et al., 2017). Modern-day Upper Crust shows a mean age of 1.8 ± 0.4 Ga (Jacobsen, 1988). While most of the Vindhyan rocks show mean ages less than 1.8 Ga, higher mean ages (> 2 Ga) are observed in some samples, which suggests that significantly older crust was exposed and subjected to erosion during sedimentation in the Vindhyan Basin (Fig. 6).

Trace element compositions of siliciclastic rocks from the CVV broadly overlap with those of stratigraphically equivalent rocks from the SVV (barring Kaimur Group), confirming the general notion that these two sub-basins are part of the large Vindhyan Basin. However, Nd isotopic compositions suggest that the siliciclastic horizons of the SVV and CVV sub-basins have not always received detritus from similar sources. It may be possible that in a large sedimentary basin, siliciclastic sediments are derived from distinct provenances and sediments from these distinct sources do not mix as they get deposited in the same stratigraphic horizon. In contrast to siliciclastic rocks, the compositions of carbonates from the same stratigrapic unit are expected to be more homogeneous and reflect the composition of the water mass from which they precipitated.

4.2. Epeiric nature of the Vindhyan Sea: Evidence from REY and Y/Ho of Vindhyan carbonates

The compositions of carbonate samples exposed both in the CVV and SVV sub-basins are analysed and their compositions are interpreted in terms of paleo-depositional environments of the Vindhyan carbonates. Prior to inferring the paleo-depositional environment of the Vindhyan carbonates using geochemical constraints, the effects of detrital contamination and diagenesis on the geochemical compositions of the carbonate rocks need to be evaluated. For the carbonate samples of the present study, detrital contamination is expected to be insignificant as the samples were dissolved using acetic acid, which selectively dissolves the carbonate phases and not the associated silicate phases. This argument is consistent with the low concentrations of Zr (< 0.2 ppm), Hf (<0.03 ppm), Sc (<4 ppm), and Th (<2 ppm) in these carbonate rocks (Table S2), which are commonly associated with detrital phases. The effect of diagenesis on the REY pattern of these limestones during stages of dolomitization was also evaluated. Although, it has been suggested that "fabric destructive" dolomitization does not modify the REY signature of limestones (Hood et al., 2018), Fe and Mn concentrations increase significantly whereas Sr concentration decreases (e.g., Derry et al., 1992). Elemental ratios such as Mn/Sr and Fe/Sr have been used to evaluate the extent of diagenesis in limestones (e.g.,Kumar et al., 2002; Ray et al., 2003). The Vindhyan carbonates from both SVV and CVV mostly show low Mn/Sr (0.4 to 8.6), and these values are within ranges recommended for unaltered limestones. The exceptions are three severely dolomitized samples (RV8A, RV8B, Bhagwanpura) from the Bhagwanpura Formation and one sample from the Bhander Formation (LBLT1–2), which show high Mn/Sr (21.9–47.1) and Fe/Sr (41.1–140.2) (Table S2). Overall, Mn/Sr and Fe/Sr ratios in the Vindhyan carbonates do not show any systematic variations with their REY compositions (figure not shown) which suggests that the REY compositions of the samples of this study have not been affected by diagenesis and can be used for inferring paleo-depositional conditions.

Modern-day seawater shows non-redox sensitive REY anomalies accompanied by super-chondritic Y/Ho ratio (>45) (Alibo and Nozaki, 1999). In comparison, modern river and lake water show lower Y/Ho (<45) and absence of positive La and Gd anomaly (Bolhar and Vankranendonk, 2007; Leybourne and Johannesson, 2008). Chemical sedimentary rocks preserve the REY behaviour of the water from which they precipitate. For example, modern marine chemical precipitates show positive La and Y anomalies, negative Ce anomaly, HREE enrichment over LREEs, and superchondritic Y/Ho ratio (Webb and Kamber, 2000), which are characteristic features of modern seawater, while chemical precipitates deposited from freshwater lack the characteristic REY signature and superchondritic Y/Ho ratio of seawater (Bolhar and Vankranendonk, 2007). This information has been widely applied to understand paleo-depositional settings (i.e., distance from the paleo-shoreline) of ancient sedimentary deposits (Frimmel, 2009) as well as to infer the paleo-tectonic settings of ancient carbonates (Zhang et al., 2017).

The PAAS normalized REY pattern of the Vindhyan carbonates from both CVV and SVV do not show signatures of modern-day seawater (Fig. 7). Specifically, the Vindhyan carbonates lack non-redox sensitive anomalies of La, Gd, and Y, which are primarily controlled by

complexation processes and are characteristic signatures of seawater (Fig. 7, Table. S2). Addtionally, in plots of $La/La^*_{(SN)}$ versus Y/Ho and $La/La^*_{(SN)}$ versus $Gd/Gd^*_{(SN)}$, the compositions of the Vindhyan carbonates do not overlap with those of modern seawater or modern and Archean marine carbonates (Fig. 8). The REY signature and Y/Ho ratio of the Vindhyan carbonates suggest precipitation from a water mass which shows significant influence of freshwater and with limited connection to the open ocean, most likely an epicontinental setting. The inferences of this study based on geochemical compositions of the Vindhyan carbonates are in contrast to some studies but are consistent with several other sedimentological studies. While some sedimentological studies suggest that some Vindhyan carbonates were deposited in a shallow marine environment (Chakraborty, 2006), other studies suggested that they were deposited in a subtidal to intertidal depositional setting (Aktar, 1996). However, our inference is consistent with the widespread global occurrence of the epeiric deposits in the Mesoproterozoic era (Gilleaudeau and Kah, 2013; Kah et al., 2012).

4.3. Inter-basinal correlation: The Nd, Ca isotopic evidence

Based on the similarity in the lithostratigraphic successions, it has been suggested the CVV and SVV sub-basins were connected (e.g., Prasad, 1984). In contrast, based on the difference in $\delta^{13}C$ values of carbonates from these two sub-basins, it has been argued that the two sub-basins were disconnected during the entire depositional history of the basin (Kumar et al., 2002; Ray et al., 2003). In the absence of body fossils, carbon isotope stratigraphy can be a valuable tool for stratigraphic correlation and has been successfully applied to the study of late Neoproterozoic carbonates, which are characterized by high-amplitude $\delta^{13}C$ fluctuations (Halverson et al., 2005). In contrast to the Neoproterozoic carbonates, $\delta^{13}C$ variability in Mesoproterozoic age carbonates is relatively "muted" (Kah et al., 2012), which limits its usability for stratigraphic correlation. Additional complexities arise in the case of epiconentinental (epeiric seas) deposits, like the Vindhyan carbonates of this study, as the nature of the carbon cycle in the restricted environments of the epeiric seas is not well resolved (Gilleaudeau and Kah, 2013; Holmden et al., 1998). Large $\delta^{13}C$ variations are observed in carbonates precipitated in restricted environments because the longer residence time and shallow water condition enhances the influence of isotopically distinct sources of carbon (e.g., Holmden et al., 1998; Kah et al., 2012). Also, it has been suggested that changes in the eustatic sea level drives the local carbon cycle in an epeiric sea environment and systematic variations in $\delta^{13}C$ with sea-level fluctuations has been documented in Palaeozoic successions (Fanton and Holmden, 2007). Given the above-mentioned complexities in interpreting the carbon isotopic composition of Paleoproterozoic and Mesoproterozoic carbonates, the difference in $\delta^{13}C$ values of carbonates from the SVV and CVV sub-basins does not necessarily mean that they were disconnected, as interpreted by Kumar et al. (2002) and Ray et al. (2003). Alternatively, the contrasting $\delta^{13}C$ composition of the carbonates from these two sub-basins could be explained by variations in the local carbon cycle and primary productivity in the near vicinity of these two sub-basins and is consistent with $\delta^{13}C_{org}$ in samples from these two sub-basins which suggest variable productivity during deposition (Kumar et al., 2005). Overall, the application of carbon isotopes for evaluating the correlation between the CVV and SVV might not be robust as the C isotope variability observed in these two sub-basins can also be explained by intrabasinal heterogeneity and varying depositional environment (Gilleadeau et al., 2018). Differences in $^{87}Sr/^{86}Sr$ of carbonates from the SVV and CVV have also been interpreted as lack of connectivity between these two sub-basins (Kumar et al., 2002). However, Sr isotope stratigraphy also has its limitations, especially when the samples show diagenetic overprint or dolomitization (Ray et al., 2003).

In this study, a combined Nd and Ca isotopic approach has been taken to further evaluate the connectivity of the two Vindhyan sub-basins. Neodymium is a non-conservative element in the seawater, which exists mostly in the dissolved form (90–95%), and the $\varepsilon_{Nd(0)}$ of the modern ocean ranges from −1 to −20 (Tachikawa, 2003). As the residence time of Nd in the seawater (~500 yr) (Tachikawa, 2003) is much shorter than seawater mixing timescales (~1500 yr), the $\varepsilon_{Nd(0)}$ value of seawater varies from one ocean basin to another, which makes it an ideal tracer of water mass mixing and has been widely used to study paleo-ocean circulation and connectivity (e.g., Scher and Martin, 2006). The $\varepsilon_{Nd(1.72\ Ga)}$ values of the purportedly correlated Kajrahat and Bhagwanpura limestones from the Semri Group overlap (Fig. 9) but show unradiogenic Nd isotopic composition compared to contemporaneous seawater Nd isotopic composition (Fig. 9). The $\varepsilon_{Nd(1.72\ Ga)}$ composition recorded by the Vindhyan carbonates show similarity with surrounding sedimentary rocks (Fig. 9). This scenario is expected in an epeiric setting where boundary exchange processes such as sediment-water interaction prevails and changes Nd isotopic composition of the water-mass. The Nd isotopic similarity suggests that the CVV and SVV sub-basins were connected and the Vindhyan Sea evolved as a well-mixed narrow passage of water.

Compared to the Kajrahat and Bhagwanpura limestones, the overlying Rohtas and Nimbahera limestones of the Lower Vindhyan show more radiogenic $\varepsilon_{Nd(1.6\ Ga)}$ (Fig. 9). A shift towards more radiogenic composition recorded in carbonates from both sub-basins is possible only if the two sub-basins were connected. Detritus composition of SVV overlaps with Rohtas Limestone. Interestingly, the $\varepsilon_{Nd(1.6\ Ga)}$ of the Rohtas Limestone also overlaps with that of porcellanites from the SVV (Chakrabarti et al., 2007a). The $\varepsilon_{Nd(1.6\ Ga)}$ of Rohtas Limestone does not overlap with that of the contemporaneous seawater (Fig. 9) suggesting the boundary exchange processes prevailed at the SVV. In contrast, in the CVV the Nimbahera Limestone show similar $\varepsilon_{Nd(1.6\ Ga)}$ as that of contemporaneous seawater (Fig. 9). Few clastic rocks from CVV show overlapping $\varepsilon_{Nd(1.6\ Ga)}$, however, one Nimbahera Limestone (RV 6B) recorded radiogenic $\varepsilon_{Nd(1.6\ Ga)}$ composition compared to CVV clastic rocks. The $\varepsilon_{Nd(1.6\ Ga)}$ composition of this sample is even more radiogenic than the contemporaneous seawater suggesting CVV water-mass received solute from juvenile sources. We suggest that the Nimbahera Limestone reflects the composition of the ancient water mass which rendered this composition due to an Andean-arc type volcanism during Lower Vindhyan sedimentation. Chakrabarti et al. (2007a) suggested existence of an Andean-type arc in the near vicinity of SVV while Shukla et al. (2019) argued for the presence of an extinct magmatic arc close to the site of deposition of the CVV. Young differentiated magmatic arcs would also expect to supply younger zircons in the surrounding sedimentary system which is absent in Semri Group siliciclastic rocks from CVV (McKenzie et al., 2013). In the Aravalli mountain range, there are evidences of Paleoproterozoic Andean-arc type magmatism (Kaur et al., 2009) but $\varepsilon_{Nd(1.6\ Ga)}$ composition of these continental arc granitoids are far more unradiogenic compared to the ~1.6 Ga Nimbahera carbonates (Fig. 5). Hence, Aravalli continental arc volcanism was unlikely to be the source of Nd to the CVV water-mass. The Andean-arc type volcanism in the vicinity of the SVV remains as most dominant source of Nd to the Vindhyan water-mass around 1.6 Ga. Few Nimbahera Limestone samples from the CVV show unusually radiogenic $\varepsilon_{Nd(t)}$ with values higher than those of the porcellanites from the SVV which is possibly due to the limited data for the SVV porcellanites and might reflect a sampling bias (Fig. 9). There is also possibility of presence of a mafic body which was supplying radiogenic Nd to the Chambal water-mass, which was not detected in the Chambal Valley detrital zircon record. However, in that case, Nimbahera carbonates would show higher concentrations of mafic mineral associated elements and high Fe concentrations which is not the case (Table S2), suggesting that the REY source was not mafic in nature. The possibility of aeolian input in both the sub-basins as a result of the Andean type arc volcanism is ruled out as large aeolian inputs would have resulted in stratified ash deposits, which are not reported from Rohtas and Nimbahera limestones. Hence, this shift in radiogenic $\varepsilon_{Nd(1.6\ Ga)}$

compositions of Rohtas and Nimbahera limestones can only be explained by sub-basin connectivity. In this scenario, Son-Valley Andean arc supplied volcaniclastic materials with radiogenic Nd isotopic composition and water-mass from both sub-basins recorded this signature. This evidence suggests during Lower Vindhyan sedimentation, the two sub-basins were connected. It is important to note that although a shift towards more radiogenic Nd isotopic composition has been recorded in both sub-basins, absolute $\varepsilon_{Nd(t)}$ values of acetic acid leached samples of Rohtas (−5.1) and Nimbahera Limestone (−0.3 to +1.6) are different (Fig. 9). It is possibly that during deposition of these carbonates around 1.6 Ga, the Vindhyan Sea had become extensive in nature; the SVV carbonate recorded shallow-water signatures while the CVV carbonate recorded a deeper water signature. This observation suggests inefficient water-mass mixing which is possible under an epeiric setting due to absence of strong currents.

The $\varepsilon_{Nd(0.9\ Ga)}$ compositions of the Upper Vindhyan Lakheri Limestone from the CVV and Bhander Limestone from the SVV overlap and is less radiogenic compared to the underlying Nimbahera and Rohtas limestones, respectively (Fig. 9). The $\varepsilon_{Nd(0.9\ Ga)}$ compositions of the Lakheri and Bhander limestones show similarity with $\varepsilon_{Nd(0.9\ Ga)}$ composition of clastic rocks of the Upper Vindhyan (Fig. 9) suggesting significant contribution from detritus. The $\varepsilon_{Nd(0.9\ Ga)}$ of contemporaneous seawater is more radiogenic in composition than the Upper Vindhyan carbonates. One sample from SVV (Maihar 3) overlaps with contemporaneous seawater but the possibility of seawater incursion in the SVV is ruled out based on the basin physiography (Ray et al., 2003). Due to this overlapping $\varepsilon_{Nd(0.9\ Ga)}$ signature we conclude the two sub-basins were connected during the deposition of Upper Vindhyan.

To further explore the connectivity of the Son Valley and Chambal Valley sub-basins, stable Ca isotope compositions of the Vindhyan carbonates were measured. The residence time of Ca in the modern ocean is ~1 Ma which is larger than the ocean mixing timescale and hence Ca is expected to behave as a conservative element (Broecker and Peng, 1982). The Ca isotopic composition of the modern seawater is broadly uniform with a $\delta^{44/40}Ca_{SRM915a}$ value of 1.88 ± 0.04‰ and marine carbonates record the primary $\delta^{44/40}Ca$ composition of the seawater over the geological past (e.g., Farkaš et al., 2007). The $\delta^{44/40}Ca_{SRM915a}$ compositions of Vindhyan carbonates from both sub-basins show wide variations but fall within the range of global Precambrian carbonates of similar age (Blättler and Higgins, 2017) (Fig. 10a). Interestingly, $\delta^{44/40}Ca_{SRM915a}$ of carbonates from the SVV (0.61‰ - 0.85‰) are mostly lower than those from the CVV (0.82‰ - 1.21‰). We further evaluate cause of this compositional variation between carbonates of both sub-basins.

Minerology plays a major role in controlling $\delta^{44/40}Ca$ composition of carbonates as different carbonate minerals have variable fractionation factors when precipitating from aqueous solutions (Gussone et al., 2020). Modern aragonites show low $\delta^{44/40}Ca_{SRM915a}$ (~0.3‰) accompanied by very high Sr concentrations (~7000 ppm), while calcites display relatively high $\delta^{44/40}Ca_{SRM915a}$ (0.8–1.0‰) with Sr concentration usually less than 900 ppm (Banner, 1995; Higgins et al., 2018). Precambrian aragonites can be identified by lower $\delta^{44/40}Ca$ composition, higher Sr content and microscopic characteristics such as presence of fan fabrics (Blättler and Higgins, 2017). Modern dolomites show higher $\delta^{44/40}Ca$ compared to their precusor carbonate minerals (Higgins et al., 2018) along with variable Sr concentrations which depends on the type of dolomitizing fluid (Banner, 1995). However, the $\delta^{44/40}Ca$ composition of Precambrian dolomites overlap with that of Precambrian calcites (Blättler and Higgins, 2017). We first evaluate if mineralogy led to the Ca isotopic variation in the Vindhyan carbonates.

Presence of fan fabric (Kumar and Sharma, 2012) and high Sr concentration ~1000 ppm in the Kajrahat Limestone suggests an aragonite precursor, which is also supported by its low $\delta^{44/40}Ca_{SRM915a}$ values. Crystal fan pseudomorphs are considerably abundant in the Precambrian sedimentary environments, from the platform margin to interior of the basin, in subtidal to supratidal region (Aktar, 1996). The stratigraphically equivalent Bhagwanpura Limestone has undergone severe dolomitization as inferred from its high Mg/Ca, Mn/Sr and Fe/Sr ratios (Table S2) and the $\delta^{44/40}Ca_{SRM915a}$ of the Bhagwanpura Limestone ranges from 0.82 to 1.09, which overlaps with $\delta^{44/40}Ca_{SRM915a}$ of Neoproterozoic dolomites (~0.91) (Kasemann et al., 2005). The precursor polymorph could not be identified for Bhagwanpura Limestone. Both Rohtas and Nimbahera limestones are calcitic in nature suggesting minerology of the precipitate is not controlling the observed $\delta^{44/40}Ca$ variation (Fig. 10). Similarly, in the Upper Vindhyans, the Lakheri and Bhander limistones have similar Mg/Ca composition and are calcitic in nature suggesting minerology is not the controlling factor for the observed $\delta^{44/40}Ca$ variation (Fig. 10).

Early diagenesis can also affect the $\delta^{44/40}Ca$ of carbonates (Higgins et al., 2018). Fluid buffered versus sediment buffered diagenesis can be distinguished using $\delta^{44/40}Ca$ values and Sr concentrations of carbonates (Higgins et al., 2018). Sediment buffered diagenesis of aragonite or high-Mg calcite results in low $\delta^{44/40}Ca$ and the inherited, high Sr concentrations are retained in the carbonates (Higgins et al., 2018). In contrast fluid-buffered diagenesis yields high $\delta^{44/40}Ca$ values in carbonates but the $\delta^{44/40}Ca$ value of the carbonate reflects that of the interacting fluid, which is dominantly seawater (Higgins et al., 2018). Among the Vindhyan carbonates of the present study, the Kajrahat Limestone shows evidence of sediment-buffered diagenesis with low $\delta^{44/40}Ca$ (0.61‰) and high Sr concentration (>900 ppm, Table. S2). However, all other Vidhyan carbonates show relatively high $\delta^{44/40}Ca$ values accompanied by low Sr concentrations, which suggest that these carbonates have gone through fluid-buffered diagenesis and hence, reflect the fluid composition which can be used for inferring paleo-depositional environments. Sedimentological studies and C isotopic composition of Vindhyan carbonates suggest existence of paleo-gradient in the Vindhyan Basin where Son-Valley records shallower part while Chambal Valley represents a deeper region (Gilleaudeau et al., 2018). Presence of oolitic limestones with intraclast horizons and mega-ripples suggests high energy environment in the SVV and absence of these features suggests low energy environment in the CVV sub-basin during deposition of the Upper Vindhyan limestones (Ray et al., 2003). The observed Ca isotopic variation between the two sub-basins is most likely due to paleo-depositional setting where the shallower Son Valley received relatively higher freshwater input leading to lower $\delta^{44/40}Ca$ of the carbonates in this sub-basin (Fig. 10). In contrast, in the CVV, greater interaction with seawater resulted in higher $\delta^{44/40}Ca$ values of the carbonates (Fig. 10). The acetic acid leached Rohtas Limestone sample RHAC-1, however, shows seawater-like high Y/Ho (Table S2), which contrasts with the low $\delta^{44/40}Ca$, the latter suggesting freshwater input. This discrepancy is explained by seawater incursion in the SVV during the deposition of Rohtas Limestone, resulting in high Y/Ho, followed by early-stage fluid-buffered diagenesis under fresh-water conditions, which lowered its $\delta^{44/40}Ca$ value. As the REYs are less susceptible to diagenesis, the REY composition of the Rohtas Limestone was not modified.

5. Conclusions

(1) Geochemical composition of the siliciclastic rocks from the Chambal Valley sub-basin of the Vindhyans suggests derivation from evolved and differentiated source rocks. Neodymium isotopic compositions suggest that the Lower Vindhyan sediments in the Chambal Valley were derived from the Banded Gneissic Complex (BGC) and Berach Granitoids along with contributions from 1.82 Ga old continental arc granitoids of the Aravalli fold belt and the Hindoli mafic volcanics. For the Upper Vindhyan sediments, contributions from older basement rocks decreased significantly while Delhi Belt granitoids became the major provenance.

(2) The lack of characteristic seawater-like Y/Ho and REY signatures in Vindhyan carbonates suggests that these carbonates were not precipitated in open-ocean settings. However, the Y/Ho values in these carbonates are higher compared to modern and ancient

lacustrine and riverine systems and the presence of minor La, Gd anomalies suggest that the Vindhyan carbonates were deposited in an epeiric environment with limited connectivity with the open ocean.

(3) The $\varepsilon_{Nd(t)}$ composition of the Vindhyan carbonates suggest the SVV and CVV sub-basins were connected during deposition of Upper and Lower Vindhyan. The Nd isotopic compositions of Lower Vindhyan carbonates shift towards radiogenic values around 1.6 Ga ago, which is consistent with eruption of an Andean-type arc in the near vicinity. Existence of a paleo-gradient in the Vindhyan Basin is suspected, as $\varepsilon_{Nd(t)}$ values of the CVV carbonates overlap with contemporaneous seawater while in the SVV, boundary exchange processes prevailed.

(4) The range in Ca isotope variation in the lowermost carbonate horizons (Kajrahat and Bhagwanpura limestones) of the Vindhyan Basin can be explained by minerology. However, the lower $\delta^{44/40}$Ca values of the 1.6 Ga and 0.9 Ga old carbonates from the Son Valley, relative to the stratigraphically equivalent carbonates from the Chambal Valley reflect the presence of a paleo-gradient in the Vindhyan Basin. The Son Valley carbonates were formed at shallower depths and their low $\delta^{44/40}$Ca reflect greater influence of freshwater compared to the Chambal Valley carbonates.

Declaration of Competing Interest

The authors declare that they have no known competing financial or personal interests that could have influenced the work reported in this paper.

Acknowledgements

This study was partially funded by CSIR (24(0355)/18/EMR-II) to RC. We thank Dr. Mukund Sharma of BSIP, Lucknow for providing us with three Vindhyan carbonate samples. We thank Dr. Asish R. Basu, Dr. Debajyoti Paul and a third anonymous reviewer and the Associate Editor Dr. Sajeev Krishnan for their comments and suggestions.

Appendix A. Supplementary data

Supplementary data to this article can be found online at https://doi.org/10.1016/j.lithos.2021.106059.

References

Ahmad, I., Mondal, M.E.A., Bhutani, R., Satyanarayanan, M., 2018. Geochemical evolution of the Mangalwar complex, Aravalli Craton, NW India: Insights from elemental and Nd-isotope geochemistry of the basement gneisses. Geosci. Front. 9, 931–942. https://doi.org/10.1016/j.gsf.2017.07.003.

Aktar, K., 1996. Facies, sedimentation processes and environments in the Proterozoic Vindhyan Basin, India. In: Bhattacharya, A. (Ed.), Recent Advances in Vindhyan Geology Geological Society of India Memoir. 36, pp. 127–136.

Alibo, D.S., Nozaki, Y., 1999. Rare earth elements in seawater: particle association, shale-normalization, and Ce oxidation. Geochim. Cosmochim. Acta 63, 363–372. https://doi.org/10.1016/S0016-7037(98)00279-8.

Banerjee, A., Chakrabarti, R., Mandal, S., 2016. Geochemical anatomy of a spheroidally weathered diabase. Chem. Geol. 440, 124–138. https://doi.org/10.1016/j.chemgeo.2016.07.008.

Banner, J.L., 1995. Application of the trace element and isotope geochemistry of strontium to studies of carbonate diagenesis. Sedimentology 42 (5), 805–824.

Basu, A., Bickford, M.E., 2015. An Alternate Perspective on the Opening and Closing of the Intracratonic Purana Basins in Peninsular India. p. 21.

Basu, P., Chakrabarti, R., 2020. Origin and evolution of the Vindhyan Basin: a geochemical perspective. Proceedings of the Indian National Science Academy. 86. https://doi.org/10.16943/ptinsa/2020/49808.

Blättler, C.L., Higgins, J.A., 2017. Testing Urey's carbonate–silicate cycle using the calcium isotopic composition of sedimentary carbonates. Earth Planet. Sci. Lett. 479, 241–251. https://doi.org/10.1016/j.epsl.2017.09.033.

Bolhar, R., Vankranendonk, M., 2007. A non-marine depositional setting for the northern Fortescue Group, Pilbara Craton, inferred from trace element geochemistry of stromatolitic carbonates. Precambrian Res. 155, 229–250. https://doi.org/10.1016/j.precamres.2007.02.002.

Bolhar, R., Kamber, B.S., Moorbath, S., Fedo, C.M., Whitehouse, M.J., 2004. Characterisation of early Archaean chemical sediments by trace element signatures. Earth Planet. Sci. Lett. 222, 43–60. https://doi.org/10.1016/j.epsl.2004.02.016.

Brasier, M.D., Lindsay, J.F., 1998. A billion years of environmental stability and the emergence of eukaryotes: New data from northern Australia. Geology 26, 555. https://doi.org/10.1130/0091-7613(1998)026<0555:ABYOES>2.3.CO;2.

Broecker, W.S., Peng, T.H., 1982. Tracers in the Sea. Eldigio Press, New York, pp. 1–690.

Cawood, P.A., Hawkesworth, C.J., 2014. Earth's middle age. Geology 42, 503–506. https://doi.org/10.1130/G35402.1.

Chakrabarti, A., 1990. Traces and dubiotraces: examples from the so-called late Proterozoic siliciclastic rocks of the Vindhyan Supergroup around Maihar, India. Precambrian Res. 47, 141–153.

Chakrabarti, R., Basu, A., Chakrabarti, A., 2007a. Trace element and Nd-isotopic evidence for sediment sources in the mid-Proterozoic Vindhyan Basin, Central India. Precambrian Res. 159, 260–274. https://doi.org/10.1016/j.precamres.2007.07.003.

Chakrabarti, R., Abanda, P.A., Hannigan, R.E., Basu, A.R., 2007b. Effects of diagenesis on the Nd-isotopic composition of black shales from the 420 Ma Utica Shale Magnafacies. Chem. Geol. 244, 221–231. https://doi.org/10.1016/j.chemgeo.2007.06.017.

Chakraborty, C., 2006. Proterozoic intracontinental basin: the Vindhyan example. Journal of Earth System Science 115, 3–22. https://doi.org/10.1007/BF02703022.

Cullers, R.L., 2002. Implications of elemental concentrations for provenance, redox conditions, and metamorphic studies of shales and limestones near Pueblo, CO, USA. Chem. Geol. 191, 305–327. https://doi.org/10.1016/S0009-2541(02)00133-X.

Derry, L.A., Kaufman, A.J., Jacobsen, S.B., 1992. Sedimentary cycling and environmental change in the late Proterozoic: evidence from stable and radiogenic isotopes. Geochim. Cosmochim. Acta 56, 1317–1329. https://doi.org/10.1016/0016-7037(92)90064-P.

Fanton, K.C., Holmden, C., 2007. Sea-level forcing of carbon isotope excursions in epeiric seas: implications for chemostratigraphy. Can. J. Earth Sci. 44, 807–818. https://doi.org/10.1139/e06-122.

Farkaš, J., Buhl, D., Blenkinsop, J., Veizer, J., 2007. Evolution of the oceanic calcium cycle during the late Mesozoic: evidence from δ44/40Ca of marine skeletal carbonates. Earth Planet. Sci. Lett. 253, 96–111. https://doi.org/10.1016/j.epsl.2006.10.015.

Frimmel, H.E., 2009. Trace element distribution in Neoproterozoic carbonates as palaeoenvironmental indicator. Chem. Geol. 258, 338–353. https://doi.org/10.1016/j.chemgeo.2008.10.033.

Garcon, M., Carlson, R.W., Shirey, S.B., Arndt, N.T., Horan, M.F., Mock, T.D., 2017. Erosion of Archean continents: the Sm-Nd and Lu-Hf isotopic record of Barberton sedimentary rocks. Geochim. Cosmochim. Acta 206, 216–235. https://doi.org/10.1016/j.gca.2017.03.006.

George, B.G., Ray, J.S., 2017. Provenance of sediments in the Marwar Supergroup, Rajasthan, India: Implications for basin evolution and Neoproterozoic global events. J. Asian Earth Sci. 147, 254–270. https://doi.org/10.1016/j.jseaes.2017.07.027.

George, B.G., Ray, J.S., Shukla, A.D., Chatterjee, A., Awasthi, N., Laskar, A.H., 2018. Stratigraphy and geochemistry of the Balwan Limestone, Vindhyan Supergroup, India: evidence for the Bitter Springs δ 13 C anomaly. Precambrian Res. 313, 18–30. https://doi.org/10.1016/j.precamres.2018.05.008.

Gilleaudeau, G.J., Kah, L.C., 2013. Carbon isotope records in a Mesoproterozoic epicratonic sea: Carbon cycling in a low-oxygen world. Precambrian Res. 228, 85–101. https://doi.org/10.1016/j.precamres.2013.01.006.

Gilleaudeau, G.J., Sahoo, S.K., Kah, L.C., Henderson, M.A., Kaufman, A.J., 2018. Proterozoic carbonates of the Vindhyan Basin, India: Chemostratigraphy and diagenesis. Gondwana Res. 57, 10–25. https://doi.org/10.1016/j.gr.2018.01.003.

Gopalan, K, Kumar, A, Kumar, S, Vijayagopal, B, 2013. Depositional history of the Upper Vindhyan succession, central India: Time constraints from Pb–Pb isochron ages of its carbonate components. Precambrian Res. 233, 108–117.

Gopalan, K., Macdougall, J.D., Roy, A.B., Murali, A.V., 1990. Sm-Nd evidence for 3.3 Ga old rocks in Rajasthan, northwestern India. Precambrian Res. 48, 287–297. https://doi.org/10.1016/0301-9268(90)90013-G.

Gussone, N., Ahm, A.-S.C., Lau, K.V., Bradbury, H.J., 2020. Calcium isotopes in deep time: potential and limitations. Chem. Geol. 544, 119601.

Halla, J., van Hunen, J., Heilimo, E., Hölttä, P., 2009. Geochemical and numerical constraints on Neoarchean plate tectonics. Precambrian Res. 174, 155–162. https://doi.org/10.1016/j.precamres.2009.07.008.

Halverson, G.P., Hoffman, P.F., Schrag, D.P., Maloof, A.C., Rice, A.H.N., 2005. Toward a Neoproterozoic composite carbon-isotope record. Geol. Soc. Am. Bull. 117, 1181. https://doi.org/10.1130/B25630.1.

Higgins, J.A., Blättler, C.L., Lundstrom, E.A., Santiago-Ramos, D.P., Akhtar, A.A., Crüger Ahm, A.-S., Bialik, O., Holmden, C., Bradbury, H., Murray, S.T., Swart, P.K., 2018. Mineralogy, early marine diagenesis, and the chemistry of shallow-water carbonate sediments. Geochim. Cosmochim. Acta 220, 512–534. https://doi.org/10.1016/j.gca.2017.09.046.

Holmden, C., Creaser, R.A., Muehlenbachs, K., Leslie, S.A., Bergström, S.M., 1998. Isotopic evidence for geochemical decoupling between ancient epeiric seas and bordering oceans: Implications for secular curves. Geology 26, 567. https://doi.org/10.1130/0091-7613(1998)026<0567:IEFGDB>2.3.CO;2.

Hood, A.V.S., Planavsky, N.J., Wallace, M.W., Wang, X., 2018. The effects of diagenesis on geochemical paleoredox proxies in sedimentary carbonates. Geochim. Cosmochim. Acta 232, 265–287. https://doi.org/10.1016/j.gca.2018.04.022.

Jacobsen, S.B., 1988. Isotopic constraints on crustal growth and recycling. Earth Planet. Sci. Lett. 90, 315–329. https://doi.org/10.1016/0012-821X(88)90133-1.

Jacobsen, S.B., Pimentel-Klose, M.R., 1988. Nd isotopic variations in Precambrian banded iron formations. Geophys. Res. Lett. 15, 393–396. https://doi.org/10.1029/GL015i004p00393.

Kah, L.C., Bartley, J.K., Teal, D.A., 2012. Chemostratigraphy of the late Mesoproterozoic Atar Group, Taoudeni Basin, Mauritania: Muted isotopic variability, facies correlation,

and global isotopic trends. Precambrian Res. 200–203, 82–103. https://doi.org/10.1016/j.precamres.2012.01.011.
Kamber, B.S., Webb, G.E., 2001. The geochemistry of late Archaean microbial carbonate: implications for ocean chemistry and continental erosion history. Geochim. Cosmochim. Acta 65, 2509–2525. https://doi.org/10.1016/S0016-7037(01)00613-5.
Kasemann, S.A., Hawkesworth, C.J., Prave, A.R., Fallick, A.E., Pearson, P.N., 2005. Boron and calcium isotope composition in Neoproterozoic carbonate rocks from Namibia: evidence for extreme environmental change. Earth Planet. Sci. Lett. 231, 73–86. https://doi.org/10.1016/j.epsl.2004.12.006.
Kaur, P., Chaudhri, N., Raczek, I., Kröner, A., Hofmann, A.W., 2007. Geochemistry, zircon ages and whole-rock Nd isotopic systematics for Palaeoproterozoic A-type granitoids in the northern part of the Delhi belt, Rajasthan, NW India: implications for late Palaeoproterozoic crustal evolution of the Aravalli craton. Geol. Mag. 144, 361–378. https://doi.org/10.1017/S0016756806002950.
Kaur, P., Chaudhri, N., Raczek, I., Kröner, A., Hofmann, A.W., 2009. Record of 1.82 Ga Andean-type continental arc magmatism in NE Rajasthan, India: Insights from zircon and Sm–Nd ages, combined with Nd–Sr isotope geochemistry. Gondwana Res. 16, 56–71. https://doi.org/10.1016/j.gr.2009.03.009.
Kumar, S., 2016. Megafossils from the Vindhyan Basin, Central India: an overview. Journal of the Palaeontological Society of India 61, 273–286.
Kumar, S., Sharma, M., 2012. Vindhyan Basin, Son Valley Area, Central India: PSI field guide-4. Palaeontological Society of India 145.
Kumar, B., Das Sharma, S., Sreenivas, B., Dayal, A.M., Rao, M.N., Dubey, N., Chawla, B.R., 2002. Carbon, oxygen and strontium isotope geochemistry of Proterozoic carbonate rocks of the Vindhyan Basin, Central India. Precambrian Res. 113, 43–63. https://doi.org/10.1016/S0301-9268(01)00199-1.
Kumar, S., Schidlowski, M., Joachimski, M.M., 2005. Carbon isotope stratigraphy of the Paleo-Neoproterozoic Vindhyan Supergroup, Central India: implications for basin evolution and intrabasinal correlation. J. Palaeontol. Soc. India 50, 65–81.
Leybourne, M.I., Johannesson, K.H., 2008. Rare earth elements (REE) and yttrium in stream waters, stream sediments, and Fe–Mn oxyhydroxides: Fractionation, speciation, and controls over REE+Y patterns in the surface environment. Geochim. Cosmochim. Acta 72, 5962–5983. https://doi.org/10.1016/j.gca.2008.09.022.
Malone, S.J., Meert, J.G., Banerjee, D.M., Pandit, M.K., Tamrat, E., Kamenov, G.D., Pradhan, V.R., Sohl, L.E., 2008. Paleomagnetism and Detrital Zircon Geochronology of the Upper Vindhyan Sequence, Son Valley and Rajasthan, India: a ca. 1000Ma Closure age for the Purana Basins? Precambrian Res. 164, 137–159. https://doi.org/10.1016/j.precamres.2008.04.004.
McKenzie, N.R., Hughes, N.C., Myrow, P.M., Xiao, S., Sharma, M., 2011. Correlation of Precambrian–Cambrian sedimentary successions across northern India and the utility of isotopic signatures of Himalayan lithotectonic zones. Earth Planet. Sci. Lett. 312, 471–483. https://doi.org/10.1016/j.epsl.2011.10.027.
McKenzie, N.R., Hughes, N.C., Myrow, P.M., Banerjee, D.M., Deb, M., Planavsky, N.J., 2013. New age constraints for the Proterozoic Aravalli–Delhi successions of India and their implications. Precambrian Res. 238, 120–128. https://doi.org/10.1016/j.precamres.2013.10.006.
McLennan, S.M., Hemming, S.R., Taylor, S.R., Eriksson, K.A., 1995. Early Proterozoic crustal evolution: Geochemical and NdPb isotopic evidence from metasedimentary rocks, southwestern North America. Geochim. Cosmochim. Acta 59, 1153–1177. https://doi.org/10.1016/0016-7037(95)00032-U.
Mondal, S, Chakrabarti, R, 2018. A novel sample loading method and protocol for monitoring sample fractionation for high precision Ca stable isotope ratio measurements using double-spike TIMS. J. Anal. At. Spectrom 33, 141–150. https://doi.org/10.1039/c7ja00322f.
Mondal, M.E.A., Raza, A., 2013. Geochemistry of sanukitoid series granitoids from the Neoarchaean Berach granitoid batholiths, Aravalli craton, northwestern Indian shield. Curr. Sci. 105, 7.
Moyen, J.-F., Martin, H., 2012. Forty years of TTG research. Lithos 148, 312–336. https://doi.org/10.1016/j.lithos.2012.06.010.
Nothdurft, L.D., Webb, G.E., Kamber, B.S., 2004. Rare earth element geochemistry of late Devonian reefal carbonates, Canning Basin, Western Australia: confirmation of a seawater REE proxy in ancient limestones. Geochim. Cosmochim. Acta 68, 263–283. https://doi.org/10.1016/S0016-7037(03)00422-8.
Och, L.M., Shields-Zhou, G.A., 2012. The Neoproterozoic oxygenation event: Environmental perturbations and biogeochemical cycling. Earth Sci. Rev. 110, 26–57. https://doi.org/10.1016/j.earscirev.2011.09.004.
Paikaray, S., Banerjee, S., Mukherji, S., 2008. Geochemistry of shales from the Paleoproterozoic to Neoproterozoic Vindhyan Supergroup: Implications on provenance, tectonics and paleoweathering. J. Asian Earth Sci. 32, 34–48. https://doi.org/10.1016/j.jseaes.2007.10.002.
Pandit, M.K., Carter, L.M., Ashwal, L.D., Tucker, R.D., Torsvik, T.H., Jamtveit, B., Bhushan, S.K., 2003. Age, petrogenesis and significance of 1Ga granitoids and related rocks from the Sendra area, Aravalli Craton, NW India. J. Asian Earth Sci. 22, 363–381. https://doi.org/10.1016/S1367-9120(03)00070-1.
Planavsky, N.J., Reinhard, C.T., Wang, X., Thomson, D., McGoldrick, P., Rainbird, R.H., Johnson, T., Fischer, W.W., Lyons, T.W., 2014. Low Mid-Proterozoic atmospheric oxygen levels and the delayed rise of animals. Science 346, 635–638. https://doi.org/10.1126/science.1258410.
Prasad, B., 1984. Geology, sedimentation and paleogeography of the Vindhyan Supergroup, S.E Rajasthan. Memoirs of the Geological Survey of India 116, 1–107.
Rao, Y.H., Venkateshwarlu, M., Papanna, G., Rao, B.R., 2013. Palaeomagnetism of Khairmalia Volcanics, south of Chittorgarh – implications related to the basal age of the Proterozoic Vindhyan Supergroup. Curr. Sci. 104, 4.
Ray, J.S., Veizer, J., Davis, W.J., 2003. C, O, Sr and Pb isotope systematics of carbonate sequences of the Vindhyan Supergroup, India: age, diagenesis, correlations and implications for global events. Precambrian Res. 121, 103–140. https://doi.org/10.1016/S0301-9268(02)00223-1.
Raza, M., Dayal, A.M., Khan, A., Bhardwaj, V.R., Rais, S., 2010. Geochemistry of lower Vindhyan clastic sedimentary rocks of Northwestern Indian shield: Implications for composition and weathering history of Proterozoic continental crust. J. Asian Earth Sci. 39, 51–61. https://doi.org/10.1016/j.jseaes.2010.02.007.
Raza, M., Khan, A., Bhardwaj, V.R., Rais, S., 2012. Geochemistry of Mesoproterozoic sedimentary rocks of upper Vindhyan Group, southeastern Rajasthan and implications for weathering history, composition and tectonic setting of continental crust in the northern part of Indian shield. J. Asian Earth Sci. 48, 160–172. https://doi.org/10.1016/j.jseaes.2011.11.012.
Rudnick, R.L., Gao, S., 2003. Composition of the continental crust. In: Rudnick, R.L., Holland, H.D., Turekian, K.K. (Eds.), Treatise on Geochemistry. Elsevier, Amsterdam, pp. 1–64.
Scher, H.D., Martin, E.E., 2006. Timing and Climatic Consequences of the opening of Drake Passage. Science 312, 428–430. https://doi.org/10.1126/science.1120044.
Shukla, A.D., George, B.G., Ray, J.S., 2019. Evolution of the Proterozoic Vindhyan Basin, Rajasthan, India: insights from geochemical provenance of siliciclastic sediments. International Geology Review, 1–15 https://doi.org/10.1080/00206814.2019.1594412.
Tachikawa, K., 2003. Neodymium budget in the modern ocean and paleo-oceanographic implications. J. Geophys. Res. 108. https://doi.org/10.1029/1999JC000285.
Tandon, S.K., Pant, C.C., Casshyap, S.M., 1991. Sedimentary Basins of India—Tectonic Context. Gyanodaya Prakashan, Nainital.
Taylor, S.R., McLennan, S.M., 1985. The Continental Crust: Its Composition and Evolution. Blackwcll, Oxford (312 pp).
Tripathy, G.R., Singh, S.K., 2015. Re–Os depositional age for black shales from the Kaimur Group, Upper Vindhyan, India. Chem. Geol. 413, 63–72. https://doi.org/10.1016/j.chemgeo.2015.08.011.
Turner, C.C., Meert, J.G., Pandit, M.K., Kamenov, G.D., 2014. A detrital zircon U–Pb and Hf isotopic transect across the Son Valley sector of the Vindhyan Basin, India: Implications for basin evolution and paleogeography. Gondwana Res. 26, 348–364. https://doi.org/10.1016/j.gr.2013.07.009.
Van Kranendonk, M.J., Webb, G.E., Kamber, B.S., 2003. Geological and trace element evidence for a marine sedimentary environment of deposition and biogenicity of 3.45 Ga stromatolitic carbonates in the Pilbara Craton, and support for a reducing Archaean Ocean. Geobiology 1, 91–108. https://doi.org/10.1046/j.1472-4669.2003.00014.x.
Webb, G.E., Kamber, B.S., 2000. Rare earth elements in Holocene reefal microbialites: a new shallow seawater proxy. Geochim. Cosmochim. Acta 64, 1557–1565. https://doi.org/10.1016/S0016-7037(99)00400-7.
Zachariah, J.K., Bhaskar Rao, Y.J., Srinivasan, R., Gopalan, K., 1999. Pb, Sr and Nd isotope systematics of uranium mineralised stromatolitic dolomites from the proterozoic Cuddapah Supergroup, South India: constraints on age and provenance. Chem. Geol. 162, 49–64. https://doi.org/10.1016/S0009-2541(99)00100-X.
Zhang, K.-J., Li, Q.-H., Yan, L.-L., Zeng, L., Lu, L., Zhang, Y.-X., Hui, J., Jin, X., Tang, X.-C., 2017. Geochemistry of limestones deposited in various plate tectonic settings. Earth Sci. Rev. 167, 27–46. https://doi.org/10.1016/j.earscirev.2017.02.003.